Disentangling the spin-parity of a resonance via the gold-plated decay mode*

Tanmoy Modak[1;1)] Dibyakrupa Sahoo[1;2)] Rahul Sinha[1;3)] Hai-Yang Cheng[2;4)] Tzu-Chiang Yuan[2;5)]

[1] The Institute of Mathematical Sciences, Taramani, Chennai 600113
[2] Institute of Physics, Academia Sinica, Taipei, 11529

Abstract: Searching for new resonances and finding out their properties is an essential part of any existing or future particle physics experiment. The nature of a new resonance is characterized by its spin, charge conjugation, parity, and its couplings with the existing particles of the Standard Model. If a new resonance is found in the four lepton final state produced via two intermediate Z bosons, the resonance could be a new heavy scalar or a Z′ boson or even a higher spin particle. In such cases a step by step methodology as enunciated in this paper can be followed to determine the spin, parity and the coupling to two Z bosons of the parent particles, in a fully model-independent way. In our approach we show how three uni-angular distributions and a few experimentally measurable observables can conclusively tell us about the spin, parity as well as the couplings of the new resonance to two Z bosons. We have performed a numerical analysis to validate our approach and showed how the uni-angular observables can be used to disentangle the spin parity as well as the coupling of the resonance.

Keywords: general spin-parity analysis, angular distributions, angular asymmetries

PACS: 12.60.-i, 14.80.Ec, 14.80.-j **DOI:** 10.1088/1674-1137/40/3/033002

1 Introduction

With the recent discovery of the 'Higgs' boson [1,2], all the ingredients of the standard model of particle physics (SM) have been found. However, we do know that the SM does not fully explain the whole of nature at its most fundamental level. For example, the problem of naturalness, the existence of extremely small masses for the neutrinos required to explain the observed neutrino oscillations, the abundance of matter over anti-matter in our observable universe and the constituents of dark matter (which is about five times more abundant than the ordinary matter) are a few of many issues which cannot be handled in the SM. So the SM encompasses an incomplete description of nature and hence it must be supplemented or extended with some other hitherto unknown new physics. Any model of new physics invariably includes new interactions and thus many new particles. In order to have a comprehensive view of new physics it is therefore essential to look for new fundamental particles in experiments such as the Large Hadron Collider (LHC) or in the proposed future experiments such as the International Linear Collider (ILC), Circular Electron Positron Collider (CEPC) and Super Proton-Proton Collider (SppC) . It is however important to have model independent methods in place to characterize resonances that could be observed in these high luminosity and high energy experiments. This paper is a step forward in that direction.

A similar idea was espoused in Ref. [3] in connection with the 125–126 Gev 'Higgs' resonance. Since the 'Higgs' was found to decay to two photons, the spin-1 possibility in this case was ruled out using the Landau-Yang theorem. This paper, however, has the complete theoretical analysis and we do consider the spin-1 possibility here. The decay of a resonance to four leptons via a pair of Z bosons is considered as the gold plated mode for discovery of any resonance in a hadron collider such as LHC. This mode can be used to search for many

Received 1 September 2015
∗ Supported in part by MOST (Taiwan)(103-2112-M-001-005 (HYC), 101-2112-M-001-005-MY3 (TCY))
1) E-mail: tanmoyy@imsc.res.in
2) E-mail: sdibyakrupa@imsc.res.in
3) E-mail: sinha@imsc.res.in
4) E-mail: phcheng@phys.sinica.edu.tw
5) E-mail: tcyuan@gate.sinica.edu.tw

new resonances, such as a heavy scalar resonance, a Z′ boson or a Kaluza-Klein boson, or a massive graviton. Hence, all the spin possibilities must be considered. We analyse the decay of a resonance (say, X with spin-J) via this golden channel: $X \to Z^{(*)}Z^{(*)} \to (l_1^- l_1^+)(l_2^- l_2^+)$, where l_1, l_2 are leptons e or μ. Since we are considering an unknown particle with unknown mass, it may be heavy enough to produce two real Z bosons or we can have one on-shell Z and another off-shell Z, or both the Z's can be off-shell. We emphasize that the final state $(e^+e^-)(\mu^+\mu^-)$ is not equivalent to $(e^+e^-)(e^+e^-)$ or $(\mu^+\mu^-)(\mu^+\mu^-)$ as sometimes mentioned in the literature, since the latter final states have to be anti-symmetrized with respect to each of the two sets of identical fermions in the final state. The anti-symmetrization of the amplitudes is not done in our analysis and hence our analysis applies only to $(e^+e^-)(\mu^+\mu^-)$. Since X decays to two Z bosons which are vector bosons, X can have spin possibilities $J = 0, 1, 2$. Higher spin possibilities ($J \geqslant 3$) need not be considered, as the number of independent helicity amplitudes remains three (for higher odd integer spins) or six (for higher even integer spins), and the only change in the amplitude comes from extra powers of momentum of the Z bosons[1)]. This was shown by an example in Ref. [3]. In this paper we examine the angular distributions for the different spins $J = 0, 1, 2$ and parity of such a new resonance X and present a strategy to determine them, as well as the couplings of X to the pair of Z bosons with the help of a few well defined experimental observables.

We start by considering the most general effective Lagrangian for each spin possibility of X decaying to two Z bosons and then write down the corresponding decay vertices. We evaluate the partial decay rate of X in terms of the invariant mass squared of the dileptons produced from the two Z decays and the angular distributions of the four lepton final state. We demonstrate that by studying three uni-angular distributions (i.e. *distributions involving only one angle*) one can almost completely determine the spin and parity of X and also explore any anomalous couplings in the most general fashion. We provide some experimental observables that can be tested to predict whether the resonance is a parity eigenstate or not irrespective of its spin. Then we analyse the nuances of differences in the uni-angular distributions which we take into consideration for separating each of the spin-parity possibilities. For this we express our uni-angular distributions in terms of helicity amplitudes, in the transversity basis, which are very effective in their sensitivities to the parity of the parent particle. We find that the $J = 1$ possibility can be easily distinguished from the $J = 0, 2$ possibilities since the uni-angular distributions for $J = 1$ are completely predictable.

Nelson [4–6] and Dell'Aquilla [5] realized the significance of studying angular correlations in such processes as a Higgs ($J = 0$) boson decaying to a pair of Z bosons for inferring the nature of the Higgs boson. Refs. [7–10] were the first to extend the analysis to include higher spin possibility. We study similar angular correlations in this paper to unambiguously determine the spin and parity of any new resonance decaying to four leptons via two Z bosons. We begin the study by considering the most general XZZ vertices for $J = 0$, $J = 1$ and $J = 2$ resonance X. Then we find out the effective Lagrangians and uni-angular distributions in terms of different observables for each spin possibility and lay out a procedure to identify them. We emphasize that the full angular distribution for the decay is described in terms of orthogonal functions of the sine and cosine of the angles involved in the decay. Hence, no information is lost by considering uni-angular distributions.

The decay of a resonance into two Z bosons which then decay into four leptons has been well studied in literature for different spin possibilities. For example Refs. [11–21] as well as Refs. [7–10] extensively discuss the coupling of X to two Z bosons for different spin possibilities as well as how to determine the spin-parity of a new resonance decaying into four leptons via a pair of Z bosons. More recent references for Higgs decay to four leptons via two Z bosons can be found in Refs.[3, 18, 22–24]. The aim of the current paper should not be confused with that of Ref. [3], which dealt only with the 125 Gev Higgs case. The current paper significantly improves upon the concepts presented in Ref. [3] by generalizing them to search for new resonances of arbitrary mass and arbitrary spin-parity using the gold-plated decay mode. The analysis now includes the possibility of a spin-1 resonance which can also decay to two on-shell Z bosons, a case which was not dealt with earlier. Ref. [16] does consider the spin-1 possibility. However, we emphasize that our analysis differs from this analysis as well, in many significant aspects. Our analysis does not depend on the resonance production mechanism. Unlike Ref. [16], we start with the most general effective Lagrangian for any spin and parity possibility. Our treatment in terms of transversity amplitudes is explicit on their parity behavior whereas the amplitudes of the other reference are ambivalent. We carefully use the Schouten identity to show which specific combinations of vertex factors contribute to the orthogonal transversity amplitudes.

1). In this work we do not consider the spin-3 possibility. For the spin-3 case there would be two parity-even transversity amplitudes and one parity-odd transversity amplitude. Therefore, it can, in general, be distinguished from the spin-1 case for which we have only two transversity amplitudes, one parity-even and the other parity-odd. The spin-4 and higher spin cases are similarly not considered, because all higher even spin cases have six transversity amplitudes (the same number as the spin-2 case) and all higher odd spin cases have three transversity amplitudes (the same number as the spin-3 case).

We show numerically that the uni-angular distributions can indeed be used to disentangle the spin and parity of the resonance X. We benchmark our analysis for the $J=1$ possibility of X and calculate the values of the angular asymmetries for the 14 TeV and 33 TeV LHC runs. The analysis can also be extended for the $J=2$ spin possibility.

A few words about the notation followed in this paper are necessary. Since our aim in this paper is to get an insight into the spin and parity of the resonance under consideration, the notation has been carefully designed in such a way that at any stage in the paper one would have no difficulty in recognizing the terms (in Lagrangian or vertex factor or amplitude) which contribute for even and odd parity cases. We use $e_i^{(J)}$ ($o_i^{(J)}$), $E_i^{(J)}$ ($O_i^{(J)}$), and $A_{\mathrm{E}i}^{(J)}$ ($A_{\mathrm{O}i}^{(J)}$) for parity-even (parity-odd) coupling constants, form factors and helicity amplitudes respectively for spin-J case in general. All the notations are described when they are introduced in the paper.

Section 2 deals completely with the stepwise building of the theoretical analysis. In subsection 2.1 we write down the most general Lagrangian and corresponding vertex factor for each possible spin. Transversity amplitudes and uni-angular distributions for each of the spin possibilities are analyzed in subsections 2.2 and 2.3 respectively. In Section 3 we discuss the possibility of finding one such resonance and investigate how to disentangle them. In subsection 3.1 we find the uni-angular distributions and the values of the observables for a spin-1^+ heavy resonance in future 14 TeV and 33 TeV LHC runs. We repeat the analysis for a spin-1^- resonance in subsection 3.2. We summarize in Section 4 emphasizing the importance of our results.

2 Analysis of the decay of a resonance to four final charged leptons via two Z bosons

Let us consider the decay of X to four charged leptons via a pair of Z bosons:

$$\mathrm{X}\to \mathrm{Z}_1+\mathrm{Z}_2\to(\mathrm{l}_1^-+\mathrm{l}_1^+)+(\mathrm{l}_2^-+\mathrm{l}_2^+),$$

where l_1, l_2 are leptons e or μ. As mentioned in the introduction we assume l_1 and l_2 are not identical. The kinematics for the decay is shown in Fig. 1. The resonance X at rest decays to two Z bosons (none of them or either of them or both of them can be on-shell depending on the mass of X), Z_1 and Z_2, moving along the $+\hat{z}$ and $-\hat{z}$ directions with four-momenta q_1 and q_2 respectively. The decays of Z_1 and Z_2 are considered in their respective rest frames. The angles and momenta involved are as described in Fig. 1. The four-momentum of X is defined as P: $P=q_1+q_2$. We also define $Q=q_1-q_2$. We choose Z_1 to decay to lepton pair $\mathrm{l}_1^\pm$ with momenta k_1 and k_2 respectively and Z_2 to decay to $\mathrm{l}_2^\pm$ with momenta k_3 and k_4 respectively. We define two unit normals $\vec{n}_1$ and $\vec{n}_2$ to the planes containing $\vec{k}_1,\vec{k}_2$ and $\vec{k}_3,\vec{k}_4$ respectively by

$$\vec{n}_1=\frac{\vec{k}_1\times\vec{k}_2}{\left|\vec{k}_1\times\vec{k}_2\right|}=-\hat{y}, \tag{1}$$

$$\vec{n}_2=\frac{\vec{k}_3\times\vec{k}_4}{\left|\vec{k}_3\times\vec{k}_4\right|}=-(\sin\phi\hat{x}-\cos\phi\hat{y}). \tag{2}$$

Thus the azimuthal angle ϕ can be specified unambiguously by

$$\vec{n}_1\cdot\vec{n}_2=-\cos\phi, \tag{3}$$

$$\vec{n}_1\times\vec{n}_2=-\sin\phi\hat{z}. \tag{4}$$

We begin the study by considering the most general XZZ interaction Lagrangians for a $J=0$, a $J=1$ and a $J=2$ resonance X. From the Lagrangians we find the most general XZZ decay vertex factor for each spin possibility.

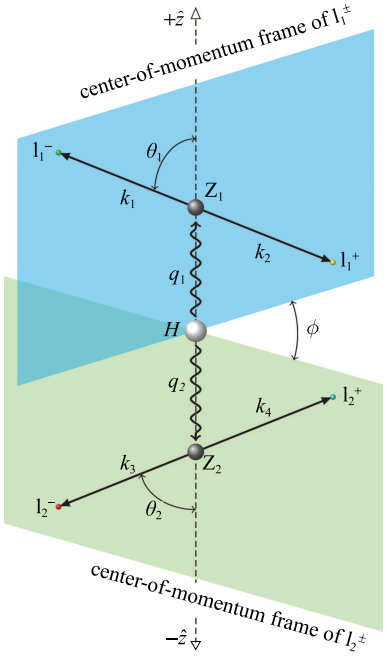

Fig. 1. (color online) Definition of the polar angles (θ_1 and θ_2) and the azimuthal angle (ϕ) in the decay of X to a pair of Z's, and then to four charged leptons: $\mathrm{X}\to\mathrm{Z}_1+\mathrm{Z}_2\to(\mathrm{l}_1^-+\mathrm{l}_1^+)+(\mathrm{l}_2^-+\mathrm{l}_2^+)$, where $\mathrm{l}_1,\mathrm{l}_2\in\{\mathrm{e},\mu\}$. It should be clear from the figure that $\vec{k}_1=-\vec{k}_2$ and $\vec{k}_3=-\vec{k}_4$. The lepton pairs are reconstructed in their respective center-of-momentum frames. The angle between the two decay planes is the angle ϕ. The spin projection of particle X is along the $\hat{z}$ direction.

2.1 Most general interaction Lagrangian and Vertex factor for the decay X → ZZ

Considering Lorentz invariance one can write down the most general interaction Lagrangian for the decay of

X to two Z bosons. The Lagrangian depends on the spin of the parent resonance X. We denote the most general Lagrangian for spin-J resonance X decaying to two Z bosons by $\mathscr{L}^{(J)}_{\rm XZZ}$. The Lagrangians for the allowed spin possibilities are given by

- $J=0$:

$$\begin{aligned}\mathscr{L}^{(0)}_{\rm XZZ} =& e^{(0)}_1\, X^{(0)}\, Z^{\alpha}\, Z^{\beta}\, g_{\alpha\beta} + e^{(0)}_2\, X^{(0)}\, Z^{\mu\nu}\, Z_{\mu\nu} \\ &+ {\rm i}\, o^{(0)}_1\, X^{(0)}\, \tilde{Z}^{\mu\nu}\, Z_{\mu\nu},\end{aligned} \tag{5}$$

- $J=1$:

$$\begin{aligned}\mathscr{L}^{(1)}_{\rm XZZ} =& o^{(1)}_1\, X^{(1)}_{\mu}\, Z^{\mu\nu}\, Z_{\nu} + o^{(1)}_2\, X^{(1)}_{\mu\nu}\, Z^{\mu}\, Z^{\nu} \\ &+ {\rm i}\, e^{(1)}_1\, X^{(1)}_{\mu}\, \tilde{Z}_{\mu\nu}\, Z^{\nu} + {\rm i}\, e^{(1)}_2\, \tilde{X}^{(1)}_{\mu\nu}\, Z^{\mu}\, Z^{\nu},\end{aligned} \tag{6}$$

- $J=2$:

$$\begin{aligned}\mathscr{L}^{(2)}_{\rm XZZ} =& e^{(2)}_1\, X^{(2)}_{\mu\nu}\, Z^{\mu}\, Z^{\nu} + e^{(2)}_2\, X^{(2)}_{\mu\nu}\, Z^{\mu\alpha}\, Z^{\nu\beta}\, g_{\alpha\beta} \\ &+ e^{(2)}_3 X^{(2)}_{\mu\nu}\, \left(\partial_{\beta} Z^{\mu\alpha}\right) \left(\partial_{\alpha} Z^{\nu\beta}\right) \\ &+ e^{(2)}_4\, \left(\partial_{\alpha}\, \partial_{\beta}\, X^{(2)}_{\mu\nu}\right) \left(Z^{\mu\alpha} Z^{\nu\beta}\right) \\ &+ e^{(2)}_5 X^{(2)}_{\mu\nu}\, \left(\partial^{\mu} Z^{\alpha\beta}\right) \left(\partial^{\nu} Z_{\alpha\beta}\right) \\ &+ {\rm i}\, o^{(2)}_1\, X^{(2)}_{\mu\nu}\, \tilde{Z}^{\mu\alpha}\, Z^{\nu\beta}\, g_{\alpha\beta} \\ &+ {\rm i}\, o^{(2)}_2\, X^{(2)}_{\mu\nu}\, \left(\partial_{\beta} \tilde{Z}^{\mu\alpha}\right) \left(\partial_{\alpha} Z^{\nu\beta}\right) \\ &+ {\rm i}\, o^{(2)}_3\, \left(\partial_{\alpha}\, \partial_{\beta}\, X^{(2)}_{\mu\nu}\right) \left(\tilde{Z}^{\mu\alpha} Z^{\nu\beta}\right) \\ &+ {\rm i}\, o^{(2)}_4\, X^{(2)}_{\mu\nu}\, \left(\partial^{\mu}\, \tilde{Z}^{\alpha\beta}\right) \left(\partial^{\nu}\, Z_{\alpha\beta}\right),\end{aligned} \tag{7}$$

where $e^{(J)}_i$ and $o^{(J)}_i$ are the effective coupling constants for a specified spin-J of the parent particle that come with the parity-even and parity-odd parts of the Lagrangian respectively; $X^{(0)}, X^{(1)}_{\mu}, X^{(2)}_{\mu\nu}$ are the scalar, vector and tensor fields for the corresponding spin possibilities of the particle X; the tensor $X^{(2)}_{\mu\nu}$ is a symmetric, traceless and divergenceless tensor; Z^{α} is the vector field for the Z boson; and $X^{(1)}_{\mu\nu}$, $\tilde{X}^{(1)}_{\mu\nu}$, $Z_{\mu\nu}$, $\tilde{Z}_{\mu\nu}$ are defined as

$$X^{(1)}_{\mu\nu} = \partial_{\mu} X^{(1)}_{\nu} - \partial_{\nu} X^{(1)}_{\mu}, \tag{8}$$

$$\tilde{X}^{(1)}_{\mu\nu} = \epsilon_{\mu\nu\rho\sigma}\, X^{(1)\rho\sigma}, \tag{9}$$

$$Z_{\mu\nu} = \partial_{\mu} Z_{\nu} - \partial_{\nu} Z_{\mu}, \tag{10}$$

$$\tilde{Z}_{\mu\nu} = \epsilon_{\mu\nu\rho\sigma}\, Z^{\rho\sigma}. \tag{11}$$

It is necessary to clearly emphasize that the two quantities $X^{(1)}_{\mu\nu}$ and $X^{(2)}_{\mu\nu}$ must not be confused. The quantity $X^{(1)}_{\mu\nu}$ is antisymmetric under the exchange of $\mu \leftrightarrow \nu$, but $X^{(2)}_{\mu\nu}$ is symmetric under the same exchange. Given the most general effective Lagrangian for each of the spin possibilities, it is imperative that one finds the effective vertex factors from it. Using the effective vertex factors one then proceeds to find the angular distributions for each of the spin possibilities, which are finally used to distinguish the different cases of spin and parity.

Analyzing the effective Lagrangians given in Eqs. (5), (6) and (7) we can write down the following vertex factors for each of the spin possibilities of X:

- $J=0$:

$$V^{\alpha\beta}_{\rm XZZ} = E^{(0)}_1\, g^{\alpha\beta} + E^{(0)}_2\, P^{\alpha} P^{\beta} + {\rm i}\, O^{(0)}_1\, \epsilon^{\alpha\beta\rho\sigma} q_{1\rho} q_{2\sigma}, \tag{12}$$

- $J=1$:

$$V^{\mu;\alpha\beta}_{\rm XZZ} = O^{(1)}_1\, \left(g^{\alpha\mu} q^{\beta}_1 + g^{\beta\mu} q^{\alpha}_2\right) + {\rm i}\, E^{(1)}_1\, \epsilon^{\alpha\beta\mu\nu}\, Q_{\nu}, \tag{13}$$

- $J=2$:

$$\begin{aligned}V^{\mu\nu;\alpha\beta}_{\rm XZZ} =& E^{(2)}_1\, \left(g^{\alpha\nu}\, g^{\beta\mu} + g^{\alpha\mu}\, g^{\beta\nu}\right) \\ &+ E^{(2)}_2 \Big(Q^{\mu}\, \left(Q^{\alpha}\, g^{\beta\nu} + Q^{\beta}\, g^{\alpha\nu}\right) \\ &\qquad + Q^{\nu}\, \left(Q^{\alpha}\, g^{\beta\mu} + Q^{\beta}\, g^{\alpha\mu}\right)\Big) \\ &+ E^{(2)}_3\, \left(Q^{\mu}\, Q^{\nu}\, g^{\alpha\beta}\right) - E^{(2)}_4\, \left(Q^{\alpha}\, Q^{\beta}\, Q^{\mu}\, Q^{\nu}\right) \\ &+ 2{\rm i}\, O^{(2)}_1 \Big(g^{\beta\nu}\, \epsilon^{\alpha\mu\rho\sigma} - g^{\alpha\nu}\, \epsilon^{\beta\mu\rho\sigma} \\ &\qquad + g^{\beta\mu}\, \epsilon^{\alpha\nu\rho\sigma} - g^{\alpha\mu}\, \epsilon^{\beta\nu\rho\sigma}\Big) q_{1\rho} q_{2\sigma} \\ &+ {\rm i}\, O^{(2)}_2 \Big(Q^{\beta}\, (Q^{\nu}\, \epsilon^{\alpha\mu\rho\sigma} + Q^{\mu}\, \epsilon^{\alpha\nu\rho\sigma}) \\ &\qquad - Q^{\alpha}\, \left(Q^{\nu}\, \epsilon^{\beta\mu\rho\sigma} + Q^{\mu}\, \epsilon^{\beta\nu\rho\sigma}\right)\Big) q_{1\rho} q_{2\sigma} \\ &+ {\rm i}\, O^{(2)}_3 \Big(\epsilon^{\alpha\beta\nu\rho} P_{\rho} Q^{\mu} + \epsilon^{\alpha\beta\mu\rho} P_{\rho} Q^{\nu}\Big) \\ &+ {\rm i}\, O^{(2)}_4\, \epsilon^{\alpha\beta\rho\sigma}\, Q^{\mu}\, Q^{\nu}\, q_{1\rho} q_{2\sigma},\end{aligned} \tag{14}$$

where $E^{(J)}_i$, $O^{(J)}_i$ are the form factors which are associated with terms that are even and odd under parity respectively, and are related to the effective coupling constants $e^{(J)}_i$, $o^{(J)}_i$ (as given in Appendix A). It is important to notice that the terms proportional to the Levi-Civita tensor $\epsilon^{\alpha\beta\mu\nu}$ are the terms that are odd under parity in the vertex factors for spin-0 and 2, but not in the case of spin 1. This can be easily explained by the fact that in the case of spin-1 there are three polarization vectors that come into the picture, which in association with the Levi-Civita tensor and the momentum Q give rise to a triple product. This triple product involves the three polarizations and is even under parity. Thus the term with the Levi-Civita tensor carries the even form factor in the case of spin-1 instead of the usual odd form factor. Moreover, the imaginary i remains with the Levi-Civita tensor to keep the vertex factor even under time reversal.

It is noteworthy that in Ref. [3], the notation used is slightly different from that used here. In order to go to the notation used in Ref. [3], the necessary substitutions are tabulated in Table 1.

The Lagrangians and vertex factors for the different spin possibilities have also been considered in the literature [7–10, 19, 25–28]. Our approach differs from these

works by isolating the parity-even and odd terms explicitly, such that the uni-angular distributions can be profitably used for characterizing the spin and parity of the particle. It is important to notice that there is no contribution from $o_2^{(1)}$ and $e_2^{(1)}$ to the vertex factors. In order to understand this let us have a look at the terms $X_{\mu\nu}^{(1)}$ and $\tilde{X}_{\mu\nu}^{(1)}$ which come in association with $o_2^{(1)}$ and $e_2^{(1)}$ respectively. Under $\mu \leftrightarrow \nu$ exchange both $X_{\mu\nu}^{(1)}$ and $\tilde{X}_{\mu\nu}^{(1)}$ pick up a relative negative sign. However, the $Z^\mu Z^\nu$ part is symmetric under the $\mu \leftrightarrow \nu$ exchange, as it should be for the case of two identical Z bosons. So considering Bose symmetry of the two daughter Z bosons, it is clear that the terms $o_2^{(1)}$ and $e_2^{(1)}$ cannot contribute, as these are overall anti-symmetric under Bose symmetry.

Table 1. The correspondence between the vertex factors of this paper with those given in Ref. [3].

spin 0	spin 2
$E_1^{(0)} \to \frac{igM_{\rm Z}}{\cos\theta_{\rm W}} a$	$E_1^{(2)} \to A$
$E_2^{(0)} \to \frac{igM_{\rm Z}}{\cos\theta_{\rm W}} b$	$E_2^{(2)} \to B$
$O_1^{(0)} \to \frac{igM_{\rm Z}}{\cos\theta_{\rm W}} c$	$E_3^{(2)} \to C$
	$E_4^{(2)} \to D$
	$O_1^{(2)} \to E$
	$O_2^{(2)} \to F$
	$O_3^{(2)} \to G$

Before we embark upon the journey to find out the differential decay rate or the uni-angular distributions, it would be nice to have some physical understanding of the process under consideration. Analysing the decay $\rm X \to ZZ$ in terms of the helicity amplitudes and partial waves offer a valuable insight to the understanding of the process.

2.2 Helicity amplitudes in the transversity basis for the decay X → ZZ

Helicity amplitudes in the transversity basis in which we are going to work have a very special property: the helicity amplitudes are now sensitive to the parity of the resonance X. Thus our helicity amplitudes have distinct and unambiguous parity signatures. We shall denote those helicity amplitudes which have parity-even form factors as $A_{{\rm E}\,i}^{(J)}$ and those with parity-odd form factors as $A_{O\,i}^{(J)}$, where the superscript (J) denotes the spin of the parent particle X. The formalism for the helicity amplitudes is discussed in Appendix B. Ignoring the lepton masses in the final state, we get the following helicity amplitudes for the different spin possibilities of X:

- $J=0$:

$$A_{\rm E1}^{(0)} = \frac{1}{2}\left(M_{\rm X}^2 - M_1^2 - M_2^2\right) E_1^{(0)} + M_{\rm X}^2 Y^2 E_2^{(0)}, \tag{15a}$$

$$A_{\rm E2}^{(0)} = \sqrt{2} M_1 M_2 E_1^{(0)}, \tag{15b}$$

$$A_{\rm O1}^{(0)} = \sqrt{2} M_1 M_2 M_{\rm X} Y O_1^{(0)}, \tag{15c}$$

- $J=1$:

$$A_{\rm O1}^{(1)} = \frac{\sqrt{2}}{3} D_1 O_1^{(1)}, \tag{16a}$$

$$A_{\rm E1}^{(1)} = \frac{1}{3} D_2 E_1^{(1)}, \tag{16b}$$

- $J=2$:

$$\begin{aligned} A_{\rm E1}^{(2)} = \frac{2\sqrt{2}}{3\sqrt{3}M_{\rm X}^2}\Big(& E_1^{(2)}\left(M_{\rm X}^4 - M_-^4\right) - E_2^{(2)}\left(8M_{\rm X}^4 Y^2\right) \\ & + E_3^{(2)}\left(4M_{\rm X}^2 Y^2\right)\left(M_+^2 - M_{\rm X}^2\right) \\ & - E_4^{(2)}\left(8M_{\rm X}^4 Y^4\right)\Big), \end{aligned} \tag{17a}$$

$$A_{\rm E2}^{(2)} = \frac{8M_1M_2}{3\sqrt{3}}\left(E_1^{(2)} + 4Y^2 E_3^{(2)}\right), \tag{17b}$$

$$\begin{aligned} A_{\rm E3}^{(2)} = \frac{4}{3M_{\rm X}M_+}\Big(& E_1^{(2)}\left(M_-^4 - M_{\rm X}^2 M_+^2\right) \\ & + E_2^{(2)}\left(4M_+^2 M_{\rm X}^2 Y^2\right)\Big), \end{aligned} \tag{17c}$$

$$A_{\rm E4}^{(2)} = \frac{8M_1M_2\nu^2}{3M_{\rm X}M_+} E_1^{(2)}, \tag{17d}$$

$$A_{\rm O1}^{(2)} = \frac{4Y}{3M_+}\left(O_1^{(2)}\left(M_-^4 - M_{\rm X}^2 M_+^2\right) + O_2^{(2)}\left(4M_+^2 M_{\rm X}^2 Y^2\right)\right), \tag{17e}$$

$$A_{\rm O2}^{(2)} = \frac{8M_1M_2\mu^2 Y}{3\sqrt{3}M_+} O_1^{(2)}, \tag{17f}$$

where $M_{\rm X}$ is the mass of the resonance X, M_1 is the invariant mass of the $\rm l_1^\pm$ lepton pair, M_2 is the invariant mass of the $\rm l_2^\pm$ lepton pair (for off-shell contributions M_1^2, M_2^2 are not equal to M_Z^2), Y is the magnitude of the three-momentum with which the two Z bosons fly away back-to-back in the rest frame of X:

$$Y = \frac{\sqrt{\lambda(M_{\rm X}^2, M_1^2, M_2^2)}}{2M_{\rm X}}, \tag{18}$$

with

$$\lambda(x,y,z) = x^2 + y^2 + z^2 - 2(xy + yz + zx), \tag{19}$$

being the Källén function, and D_1 and D_2 are given by

$$\begin{aligned} D_1^2 = & 2M_{\rm X}^6 M_+^2 - \frac{1}{2}M_{\rm X}^4\left(5M_+^4 + M_-^4\right) \\ & + 6M_{\rm X}^2\left(M_+^6 - M_+^2 M_-^4\right) + \frac{3}{2}M_+^4 M_-^4 - \frac{1}{2}M_-^8, \end{aligned} \tag{20}$$

$$\begin{aligned} D_2^2 = & 16M_{\rm X}^6 M_+^2 + 56M_{\rm X}^4 M_+^4 - 86M_{\rm X}^2 M_+^6 \\ & + M_-^4\left(-85M_{\rm X}^4 + 96M_{\rm X}^2 M_+^2 - 35M_+^4\right) + 38M_-^8, \end{aligned} \tag{21}$$

with M_+, M_-, μ^2 and ν^2 being given by

$$M_+^2 = M_1^2 + M_2^2, \tag{22}$$
$$M_-^2 = M_1^2 - M_2^2, \tag{23}$$
$$\mu^4 = 4M_{\rm X}^2 M_+^2 + 3M_-^4, \tag{24}$$
$$\nu^4 = 2M_{\rm X}^2 M_+^2 + M_-^4. \tag{25}$$

It is noteworthy that considering the vertex factors with form factors $E_1^{(2)}$, $E_2^{(2)}$, $E_3^{(2)}$, $E_4^{(2)}$, $O_1^{(2)}$ and $O_2^{(2)}$ suffice to provide the most general angular distribution for the spin-2 case. Including the form factors $O_3^{(2)}$, and $O_4^{(2)}$ result in only a redefinition of the form factors $O_1^{(2)}$ and $O_2^{(2)}$ as discussed in Appendix C.

It is again noteworthy that the amplitudes used here are notationally different from the amplitudes used in Ref. [3] for better clarity of their physical content. By following the substitutions as given in Table 2 one can go back to the notations used in Ref. [3]. The notations $M_\pm$, μ and ν have been introduced to make the power counting of mass dimensions easy.

Table 2. The correspondence between the vertex factors of this paper with those given in Ref. [3].

spin 0	spin 2
$A_{\rm E1}^{(0)} \to A_L$	$A_{\rm O1}^{(2)} \to A_L$
$A_{\rm E2}^{(0)} \to A_\parallel$	$A_{\rm O2}^{(2)} \to A_M$
$A_{\rm O1}^{(0)} \to A_\perp$	$A_{\rm E1}^{(2)} \to A_1$
	$A_{\rm E2}^{(2)} \to A_2$
	$A_{\rm E3}^{(2)} \to A_3$
	$A_{\rm E4}^{(2)} \to A_4$
	$Y \to X$
	$M_+ \to \mathsf{u}_1$
	$M_- \to \mathsf{u}_2$
	$\mu^2 \to \mathsf{v}$
	$\nu^2 \to \mathsf{w}$

2.3 Uni-angular distributions for the decay $\mathbf{X} \to \mathbf{Z}_1\ \mathbf{Z}_2 \to (\mathrm{l}_1^+\mathrm{l}_1^-)(\mathrm{l}_2^+\mathrm{l}_2^-)$

Using the helicity amplitudes defined in Eqs. (15), (16) and (17), the uni-angular distributions with respect to $\cos\theta_1$, $\cos\theta_2$ and ϕ can be written in a unified notation for all the allowed spin possibilities of X as follows:

$$\frac{1}{\Gamma_{\rm f}^{(J)}}\frac{{\rm d}^3\Gamma^{(J)}}{{\rm d}q_1^2\,{\rm d}q_2^2\,{\rm d}\cos\theta_1} = \frac{1}{2} + T_1^{(J)}\cos\theta_1 + T_2^{(J)}P_2(\cos\theta_1), \tag{26}$$

$$\frac{1}{\Gamma_{\rm f}^{(J)}}\frac{{\rm d}^3\Gamma^{(J)}}{{\rm d}q_1^2\,{\rm d}q_2^2\,{\rm d}\cos\theta_2} = \frac{1}{2} + T_1^{\prime(J)}\cos\theta_2 + T_2^{\prime(J)}P_2(\cos\theta_2), \tag{27}$$

$$\frac{2\pi}{\Gamma_{\rm f}^{(J)}}\frac{{\rm d}^3\Gamma^{(J)}}{{\rm d}q_1^2\,{\rm d}q_2^2\,{\rm d}\phi} = 1 + U_1^{(J)}\cos\phi + U_2^{(J)}\cos 2\phi + V_1^{(J)}\sin\phi + V_2^{(J)}\sin 2\phi, \tag{28}$$

where $T_i^{(J)}$, $T_i^{\prime(J)}$, $U_i^{(J)}$, and $V_i^{(J)}$ are the coefficients of $P_i(\cos\theta_1)$, $P_i(\cos\theta_2)$, $\cos(i\phi)$, and $\sin(i\phi)$ respectively with $P_i(x)$ being the i'th Legendre polynomial in x. These coefficients can easily be obtained from the uni-angular distributions by means of the following asymmetries:

$$T_1^{(J)} = \left(-\int_{-1}^{0} + \int_{0}^{+1}\right){\rm d}\cos\theta_1\,\left(\frac{1}{\Gamma_{\rm f}^{(J)}}\frac{{\rm d}^3\Gamma^{(J)}}{{\rm d}q_1^2\,{\rm d}q_2^2\,{\rm d}\cos\theta_1}\right), \tag{29}$$

$$T_2^{(J)} = \frac{4}{3}\left(\int_{-1}^{-\frac{1}{2}} - \int_{-\frac{1}{2}}^{0} - \int_{0}^{+\frac{1}{2}} + \int_{+\frac{1}{2}}^{+1}\right){\rm d}\cos\theta_1 \times\left(\frac{1}{\Gamma_{\rm f}^{(J)}}\frac{{\rm d}^3\Gamma^{(J)}}{{\rm d}q_1^2\,{\rm d}q_2^2\,{\rm d}\cos\theta_1}\right), \tag{30}$$

$$T_1^{\prime(J)} = \left(-\int_{-1}^{0} + \int_{0}^{+1}\right){\rm d}\cos\theta_2\,\left(\frac{1}{\Gamma_{\rm f}^{(J)}}\frac{{\rm d}^3\Gamma^{(J)}}{{\rm d}q_1^2\,{\rm d}q_2^2\,{\rm d}\cos\theta_2}\right), \tag{31}$$

$$T_2^{\prime(J)} = \frac{4}{3}\left(\int_{-1}^{-\frac{1}{2}} - \int_{-\frac{1}{2}}^{0} - \int_{0}^{+\frac{1}{2}} + \int_{+\frac{1}{2}}^{+1}\right){\rm d}\cos\theta_2 \times\left(\frac{1}{\Gamma_{\rm f}^{(J)}}\frac{{\rm d}^3\Gamma^{(J)}}{{\rm d}q_1^2\,{\rm d}q_2^2\,{\rm d}\cos\theta_2}\right), \tag{32}$$

$$U_1^{(J)} = \frac{1}{4}\left(-\int_{-\pi}^{-\frac{\pi}{2}} + \int_{-\frac{\pi}{2}}^{+\frac{\pi}{2}} - \int_{+\frac{\pi}{2}}^{+\pi}\right){\rm d}\phi\,\left(\frac{2\pi}{\Gamma_{\rm f}^{(J)}}\frac{{\rm d}^3\Gamma^{(J)}}{{\rm d}q_1^2\,{\rm d}q_2^2\,{\rm d}\phi}\right), \tag{33}$$

$$U_2^{(J)} = \frac{1}{4}\left(\int_{-\pi}^{-\frac{3\pi}{4}} - \int_{-\frac{3\pi}{4}}^{-\frac{\pi}{4}} + \int_{-\frac{\pi}{4}}^{+\frac{\pi}{4}} - \int_{+\frac{\pi}{4}}^{+\frac{3\pi}{4}} + \int_{+\frac{3\pi}{4}}^{+\pi}\right){\rm d}\phi \times\left(\frac{2\pi}{\Gamma_{\rm f}^{(J)}}\frac{{\rm d}^3\Gamma^{(J)}}{{\rm d}q_1^2\,{\rm d}q_2^2\,{\rm d}\phi}\right), \tag{34}$$

$$V_1^{(J)} = \frac{1}{4}\left(-\int_{-\pi}^{0} + \int_{0}^{+\pi}\right){\rm d}\phi\,\left(\frac{2\pi}{\Gamma_{\rm f}^{(J)}}\frac{{\rm d}^3\Gamma^{(J)}}{{\rm d}q_1^2\,{\rm d}q_2^2\,{\rm d}\phi}\right), \tag{35}$$

$$V_2^{(J)} = \frac{1}{4}\left(\int_{-\pi}^{-\frac{\pi}{2}} - \int_{-\frac{\pi}{2}}^{0} + \int_{0}^{+\frac{\pi}{2}} - \int_{+\frac{\pi}{2}}^{+\pi}\right){\rm d}\phi \times\left(\frac{2\pi}{\Gamma_{\rm f}^{(J)}}\frac{{\rm d}^3\Gamma^{(J)}}{{\rm d}q_1^2\,{\rm d}q_2^2\,{\rm d}\phi}\right). \tag{36}$$

The differential decay width $\Gamma_{\rm f}^{(J)}$ is defined as

$$\Gamma_{\rm f}^{(J)} = \frac{{\rm d}^2\Gamma^{(J)}}{{\rm d}q_1^2\,{\rm d}q_2^2} = \mathscr{N}^{(J)}\left(\sum_i\left|A_{Ei}^{(J)}\right|^2 + \sum_j\left|A_{Oj}^{(J)}\right|^2\right) \tag{37}$$

where the factor $\mathscr{N}^{(J)}$ is given by

$$\mathscr{N}^{(J)} = S^{(J)}\frac{9}{2^{10}}\frac{1}{\pi^4}\frac{Br_{\rm ll}^2}{M_{\rm X}^2}\frac{\Gamma_{\rm Z}^2}{M_{\rm Z}^2}Y\frac{1}{\left(q_1^2 - M_{\rm Z}^2\right)^2 + M_{\rm Z}^2\Gamma_{\rm Z}^2} \times\frac{1}{\left(q_2^2 - M_{\rm Z}^2\right)^2 + M_{\rm Z}^2\Gamma_{\rm Z}^2}, \tag{38}$$

with $S^{(J)}$ being the factor that comes from summing over initial spin states, i.e. $S^{(J)}=1,\frac{1}{3},\frac{1}{5}$ for scalar, vector and tensor resonances respectively, $\Gamma_{\rm Z}$ being the total decay width of the Z boson, $Br_{\rm ll}$ being the branching ratio for the decay of Z to a pair of charged leptons: $\rm Z\to l^+l^-$. The coefficients $T_i^{(J)}$, $T_i^{\prime(J)}$, $U_i^{(J)}$, $V_i^{(J)}$ introduced in Eqs.(26), (27), (28) are expressed in terms of *helicity fractions* $F_{Ei}^{(J)}$ and $F_{Oi}^{(J)}$ which are defined as

$$\left.\begin{aligned} F_{Ei}^{(J)} &= \frac{A_{Ei}^{(J)}}{\sum\limits_i \left|A_{Ei}^{(J)}\right|^2+\sum\limits_j \left|A_{Oj}^{(J)}\right|^2},\\ F_{Oi}^{(J)} &= \frac{F_{Oi}^{(J)}}{\sum\limits_i \left|F_{Ei}^{(J)}\right|^2+\sum\limits_j \left|F_{Oj}^{(J)}\right|^2}, \end{aligned}\right\} \tag{39}$$

such that

$$\sum_i \left|F_{Ei}^{(J)}\right|^2+\sum_j \left|F_{Oj}^{(J)}\right|^2=1. \tag{40}$$

The expressions for the coefficients $T_i^{(J)}$, $T_i^{\prime(J)}$, $U_i^{(J)}$, $V_i^{(J)}$ are given in Appendix D. Looking at the uni-angular distributions it is easy to find that for any spin case, the coefficients $T_1^{(J)}$, $T_1^{\prime(J)}$, $V_1^{(J)}$ and $V_2^{(J)}$ are the interference terms between the parity-even and parity-odd terms. So if the resonance X were to be a parity eigenstate, these interference terms must vanish irrespective of the spin of X. Therefore, the conditions for X to be a parity eigenstate are

$$T_1^{(J)}=T_1^{\prime(J)}=V_1^{(J)}=V_2^{(J)}=0. \tag{41}$$

Now it is again easy to observe that for the spin-0 case the coefficients $T_2^{(0)}$ and $T_2^{\prime(0)}$ are the same. However this is not true for the spin-1 and spin-2 cases, in general. In order to further analyse this situation we define the difference $\Delta^{(J)}$ between $T_2^{(J)}$ and $T_2^{\prime(J)}$:

$$\Delta^{(J)}=T_2^{(J)}-T_2^{\prime(J)}. \tag{42}$$

For the different spin possibilities we have

$$\Delta^{(0)}=0, \tag{43}$$

$$\Delta^{(1)}=6M_{\rm X}^2M_-^2Y^2\left(\frac{\left|F_{O1}^{(1)}\right|^2\left(M_{\rm X}^2+M_+^2\right)}{D_1^2} + \frac{2\left|F_{E1}^{(1)}\right|^2\left(5M_{\rm X}^2+M_+^2\right)}{D_2^2}\right), \tag{44}$$

$$\begin{aligned}\Delta^{(2)}=&\frac{3M_-^2}{4M_+^2\mu^4\nu^4}\left(\mu^4\nu^4\left(\left|F_{E3}^{(2)}\right|^2+\left|F_{O1}^{(2)}\right|^2\right)\right.\\ &\left.-M_-^4\left(\mu^4\left|F_{E4}^{(2)}\right|^2+3\nu^4\left|F_{O2}^{(2)}\right|^2\right)\right)\\ &+\frac{3M_1M_2M_-^2}{M_+^2\mu^2\nu^2}\left(\mu^2\,{\rm Re}\left(F_{E3}^{(2)}F_{E4}^{(2)*}\right)\right.\\ &\left.+\sqrt{3}\nu^2\,{\rm Re}\left(F_{O1}^{(2)}F_{O2}^{(2)*}\right)\right).\end{aligned} \tag{45}$$

It is clear that we can never have $\Delta^{(1)}=0$ for all values of M_1 and M_2, since this requires $F_{E1}^{(1)}=F_{O1}^{(1)}=0$, which is an unphysical condition to satisfy as it totally obliterates the vertex factor itself. Requiring that $\Delta^{(2)}=0$ for all values of M_1 and M_2 implies that $F_{E3}^{(2)}=F_{E4}^{(2)}=F_{O1}^{(2)}=F_{O2}^{(2)}=0$, which in turn implies that $E_1^{(2)}=E_2^{(2)}=O_1^{(2)}=O_2^{(2)}=0$. Thus it leaves out two form factors in the vertex factor, namely $E_3^{(2)}$ and $E_4^{(2)}$. This case constitutes a very special case of the spin-2 scenario and all its uni-angular distributions are completely indistinguishable from the corresponding angular distributions for a parity-even spin-0 resonance. A closer look at the helicity amplitudes for these two cases, $J^P=0^+$ and special 2^+, reveals that the special 2^+ case has an extra Y^2 dependence when compared with the 0^+ case:

$$A_{E1}^{(0)}=\frac{1}{2}\left(M_{\rm X}^2-M_1^2-M_2^2\right)E_1^{(0)}+M_{\rm X}^2Y^2\,E_2^{(0)}, \tag{46}$$

$$A_{E2}^{(0)}=\sqrt{2}\,M_1\,M_2\,E_1^{(0)}, \tag{47}$$

$$A_{E1}^{(2)}=\left(-\frac{16\sqrt{2}}{3\sqrt{3}}Y^2\right)\left(\frac{1}{2}\left(M_{\rm X}^2-M_1^2-M_2^2\right)E_3^{(2)}+M_{\rm X}^2Y^2\,E_4^{(2)}\right), \tag{48}$$

$$A_{E2}^{(2)}=\left(\frac{16\sqrt{2}}{3\sqrt{3}}Y^2\right)\sqrt{2}\,M_1\,M_2\,E_3^{(2)}. \tag{49}$$

Looking at the spin-1 case we find that the coefficient $U_2^{(1)}$ is sensitive to $E_1^{(1)}$, and hence this term can be used to identify the parity of the spin-1 resonance. We can thus find a step-by-step methodology that can be followed to uniquely predict the spin and parity of a resonance decaying to four final charged leptons via two Z bosons. This is given in Fig. 2.

3 Numerical study

In this section we will show how the uni-angular distributions given in Eqs. (26), (27) and (28) can be used to find out the values of the angular observables defined in Eqs. (29), (30), (31), (32), (33), (34), (35) and (36). We shall elucidate the methodology by concentrating on some heavy spin-1 resonances and study the observables for them. We start by investigating how the mass and decay width of such resonances affect their production cross section in future LHC runs. We then benchmark the angular observables for spin-1^+ and spin-1^- resonances for two different Center-of-Momentum (CM) energies: 14 TeV and 33 TeV with 3000 fb^{-1} luminosity. This analysis can be easily extended to consider a heavy spin-2 resonance.

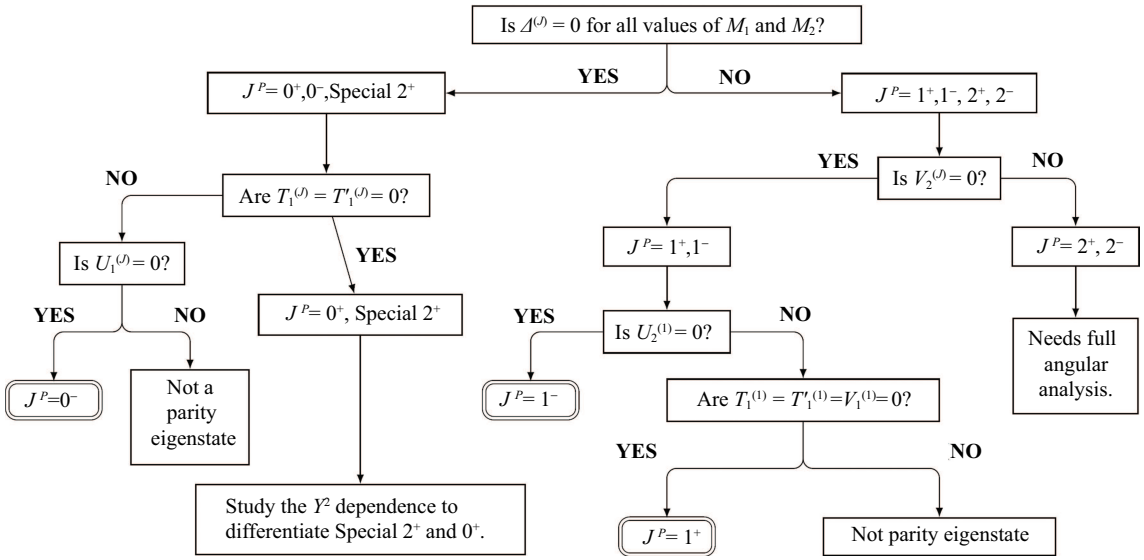

Fig. 2. Flowchart to determine the spin and parity of a resonance X decaying as $X \to Z_1 Z_2 \to (l_1^- l_1^+)(l_2^- \ell_2^+)$.

Let us consider a heavy spin-1 resonance X of mass M_X and decay width Γ_X, decaying into four charged leptons via two Z bosons. We shall assume that the resonance X is produced via annihilation of quark (q) and antiquark ($\bar{q}$) pairs. The production process is characterized by the effective Lagrangian,

$$\mathscr{L}_{\rm eff} = \sum_q (\tilde{c}_q\, \bar{q}\gamma^\mu q\, X_\mu + c_q\, \bar{q}\gamma^\mu\gamma^5 q\, X_\mu), \qquad (50)$$

where q= u, d, c, s, b quarks and $\tilde{c}_q$, c_q are the coupling strengths of X to vector, axial vector currents respectively; i.e. for a spin-1^+ resonance $\tilde{c}_q = 0$ and for a spin-1^- resonance $c_q = 0$. Just for simplicity of the analysis we have further assumed that all the quarks couple to the resonance X with the same strength. The production cross section for the resonance X can be easily obtained from Eq. (50) by considering appropriate parton distribution functions in the process $pp \to X$. The production cross section does depend on the mass of the resonance X: the larger the mass, the lower the production cross section at a given CM energy.

The decay process $X \to ZZ$ is characterized by the Lagrangian Eq. (6). The partial decay width for $X \to ZZ$ for spin-1 resonance is given by

$$\Gamma_{ZZ} = O_1^2 \frac{M_X^3}{32 M_Z^2 \pi}\left(1 - \frac{4M_Z^2}{M_X^2}\right)^{\frac{3}{2}} + E_1^2 \frac{M_X^3}{32 M_Z^2 \pi}\left(1 - \frac{4M_Z^2}{M_X^2}\right)^{\frac{5}{2}}. \qquad (51)$$

For a spin-1^+ resonance $O_1 = 0$ and for a spin-1^- resonance $E_1 = 0$. It must be noted that we have dropped the superscript "(1)" from both E_1 and O_1 throughout this section.

The partial decay width for $X \to q\bar{q}$ for a spin-1 resonance is given by

$$\Gamma_{q\bar{q}} = c_q^2 \frac{M_X}{4\pi}\left(1 - \frac{4m_q^2}{M_X^2}\right)^{\frac{3}{2}} + \tilde{c}_q^2 \frac{(M_X^2 + 2m_q^2)}{4M_X\pi}\left(1 - \frac{4m_q^2}{M_X^2}\right)^{\frac{1}{2}}, \qquad (52)$$

where m_q is the mass of the quark q (or of antiquark $\bar{q}$), and $c_q = 0$ for a spin-1^- resonance and $\tilde{c}_q = 0$ for a spin-1^+ resonance. Let us further assume that X decays to all quark-antiquark pairs and to a pair of Z bosons only, i.e. the total decay width is given by

$$\Gamma_X = \Gamma_{ZZ} + \sum_q \Gamma_{q\bar{q}}. \qquad (53)$$

One can relax these simple assumptions and do a detailed analysis where other decay channels also exist. This will lead to modifications to Eq. (53). In Fig. 3 we show how the partial decay width Γ_{ZZ} varies with the mass M_X of the spin-1^+ resonance, with $M_Z \ll M_X$. The spin-1^- resonances also exhibit a similar plot for $M_Z \ll M_X$.

One possibility for a heavy spin-1 resonance is a heavy Z′ boson. The current limit on the mass of a heavy Z′ resonance is 1.7 Tev [29]. The current limit of $\tilde{c}_q$ and c_q for a particular mass M_X of the resonance X, can be extracted out from the $\sigma \times Br \times \mathcal{A}$ vs. resonance mass (M_X) plot of Ref. [29], where σ is the cross section for the process $pp \to X$, Br is the branching fraction of the decay $X \to q\bar{q}$ and $\mathcal{A}$ is the acceptance. Since the analysis of Ref. [29] deals with the search for a heavy resonance Z′ decaying to di-jet, which is an isotropic decay (two body final state), the acceptance $\mathcal{A}$ is approximately 0.6 and is independent of the mass of Z′.

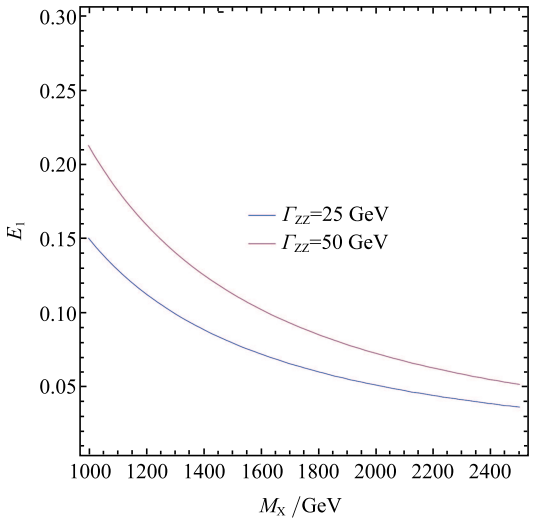

Fig. 3. (color online) Mass (M_X) vs. E_1 plot of a spin-1^+ resonance for different Γ_{ZZ}. The blue curve is for $\Gamma_{ZZ} = 25$ and the purple curve for $\Gamma_{ZZ} = 50$.

Following the analysis of Ref. [29] we find the allowed region for the couplings c_q and E_1 for two different masses, $M_X = 1.8$ TeV and 2 TeV, shown in Figs. 4 and 5 respectively. From the allowed regions shown in Figs.4 and 5, we choose three benchmark scenarios for masses $M_X = 1.8$ TeV and $M_X = 2.0$ TeV for our numerical study. The benchmark values of c_q and E_1 corresponding to both the masses are tabulated in Table 3.

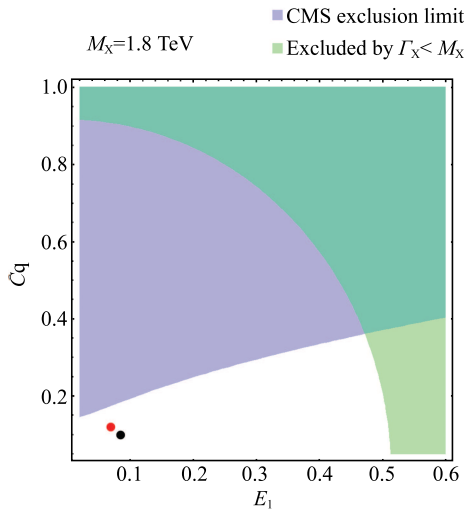

Fig. 4. (color online) The allowed region for the couplings c_q and E_1 for a spin-1^+ resonance of mass $M_X = 1.8$ TeV. The green and the blue regions are excluded by $\Gamma_X < M_X$ limit and CMS limit from Ref. [29] respectively. The red ($E_1 = 7.00 \times 10^{-2}, c_q = 0.12$) and the black ($E_1 = 8.56 \times 10^{-2}, c_q = 0.10$) dots are the two benchmark points for our analysis.

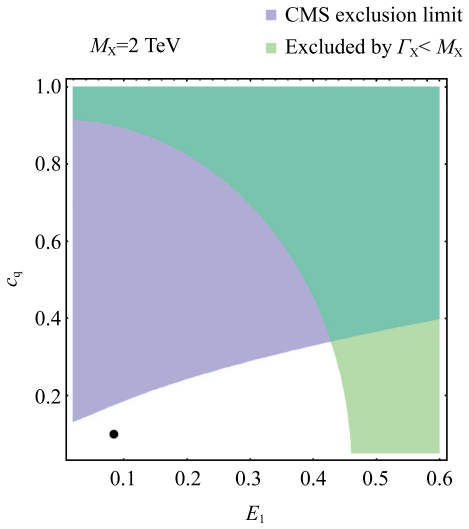

Fig. 5. (color online) The allowed region for the couplings c_q and E_1 for a spin-1^+ resonance of mass $M_X = 2$ TeV. The green and the blue regions are excluded by $\Gamma_X < M_X$ limit and CMS limit respectively. The black dot ($E_1 = 8.56 \times 10^{-2}$, $c_q = 0.10$) is the benchmark point for our analysis.

Table 3. The benchmark values of the couplings c_q and E_1 are listed for spin-1^+ resonances of masses 1.8 TeV and 2 TeV respectively for our analysis. The values of the corresponding decay widths Γ_X are also tabulated in the last column for both the masses.

mass/TeV	coupling c_q	coupling E_1	Γ_X/GeV
1.8	0.12	7.00×10^{-2}	64.40
1.8	0.10	8.56×10^{-2}	71.52
2.0	0.10	8.56×10^{-2}	92.84

Once the values of M_X, c_q(or $\tilde{c_q}$) and E_1(or O_1) for a spin-1^+ (or spin-1^-) resonance are chosen, the total decay width Γ_X as well as the cross section for the process $pp \to X \to ZZ \to e^+e^-\mu^+\mu^-$ get fixed. The reader should note that the process under consideration is within the narrow width approximation where $\Gamma_X \ll M_X$.

For event generation we used the MADEVENT5 [30] event generator interfaced with PYTHIA6.4 [31] and Delphes 3 [32]. The events are generated by pp collisions via $q\bar{q} \to X$, for the CM energies $\sqrt{s} = 14$ TeV and 33 TeV, using the parton distribution functions CTEQ6L1 [33]. Triggers as well as electron and muon identification cuts are set following the analysis presented in Refs. [34,35]. We have only selected events with final states $e^+e^-\mu^+\mu^-$, as our analysis is applicable only to four non-identical final state leptons. We have kept the trigger values the same as those for 14 TeV, for the 33 TeV LHC analysis. However, it should be noted that in the future 33 TeV LHC run, the trigger values may change,

Table 4. Effects of the sequential cuts on the simulated events at 14 TeV 3000 fb^{-1} LHC for different values of $M_{\rm X}$ and $\Gamma_{\rm X}$ of a spin-1$^+$ resonance. It is easy to observe from the benchmark scenarios considered in this table that at a given CM energy the production cross section decreases with increase in $M_{\rm X}$ and for a fixed value of $M_{\rm X}$ the production cross section decreases as the value of the decay width $\Gamma_{\rm X}$ increases.

cuts / GeV	$M_{\rm X}=1.8$ TeV, $\Gamma_{\rm X}=64.40$ GeV	$M_{\rm X}=1.8$ TeV, $\Gamma_{\rm X}=71.52$ GeV	$M_{\rm X}=2$ TeV, $\Gamma_{\rm X}=92.84$ GeV
Selection cuts	231	216	111
$60<m_{\rm ee}<120$	231	216	111
$60<m_{\mu\mu}<120$	222	208	106
$1000<m_{4\rm l}$	221	207	106

which could further improve the statistics. The electron (muon) must satisfy $E_{\rm T}>7$ GeV ($p_{\rm T}>6$ GeV) and the pseudo-rapidity cut for electron (muon) is $|\eta|<2.47$ ($|\eta|<2.7$). The leptons are required to be separated from each other by $\Delta R>0.1$ if they are of the same flavour and $\Delta R>0.2$ otherwise. The invariant mass cuts that are applied in our analysis are 60 GeV $<m_{\rm ee}<$ 120 GeV, 60 GeV $<m_{\mu\mu}<$ 120 GeV and 1000 GeV $<m_{4\rm l}$.

The effects of mass $M_{\rm X}$ and width $\Gamma_{\rm X}$ on $\sigma\times Br$ are shown in Table 4 for a spin-1$^+$ resonance. The statistics decrease as the resonance gets heavier. However, the statistics improve for a resonance with the same mass but narrower decay width. This dependence is easily discernible in Table 4 for a spin-1$^+$ resonance. This mass and width dependence on the cross sections for the $pp\to X\to ZZ\to e^+e^-\mu^+\mu^-$ process also shows the same behavior for a spin-1$^-$ resonance in the limit $m_{\rm q}\ll M_{\rm X}$ and $M_{\rm Z}\ll M_{\rm X}$.

So far we have not discussed the background for the $pp\to X\to e^+e^-\mu^+\mu^-$ process. This is discussed in the following subsection.

3.1 Study of the angular asymmetries for a spin-1$^+$resonance

In this subsection we discuss the uni-angular distributions and show how to extract the angular observables from them for a spin-1$^+$ resonance of mass $M_{\rm X}=1.8$ TeV and decay width $\Gamma_{\rm X}=64.40$ GeV. We choose this benchmark scenario as the statistics are higher for this than the other cases. We analyse the angular observables for this benchmark scenario for two different CM energies 14 TeV and 33 TeV at an integrated luminosity 3000 fb^{-1} in future LHC runs. The values of the couplings for this benchmark scenarios are $c_{\rm q}=0.12$ and $E_1=7.00\times10^{-2}$. The effects of the sequential cuts for the benchmark scenarios are tabulated in Table 5. The three uni-angular distributions for a spin-1$^+$ resonance, $\frac{1}{\Gamma}\frac{{\rm d}\Gamma}{{\rm d}\cos\theta_1}$ vs. $\cos\theta_1$, $\frac{1}{\Gamma}\frac{{\rm d}\Gamma}{{\rm d}\cos\theta_2}$ vs. $\cos\theta_2$ and $\frac{1}{\Gamma}\frac{{\rm d}\Gamma}{{\rm d}\phi}$ vs. ϕ are shown in Figs.6, 7 and 8 respectively. It should be noted that the uni-angular distributions cover the full kinematic ranges for the three variables $\cos\theta_1$, $\cos\theta_2$ and ϕ.

Table 5. The effects of the sequential cuts on the simulated signal events at 14 TeV and 33 TeV LHC with 3000 fb^{-1} luminosity for a spin-1$^+$resonance with $M_{\rm X}=1.8$ TeV and width $\Gamma_{\rm X}=$ 64.40 GeV.

cuts / GeV	14 TeV, 3000 fb^{-1}	33 TeV, 3000 fb^{-1}
Selection cuts	231	1212
$60<m_{\rm ee}<120$	231	1212
$60<m_{\mu\mu}<120$	222	1159
$1000<m_{4\rm l}$	221	1154

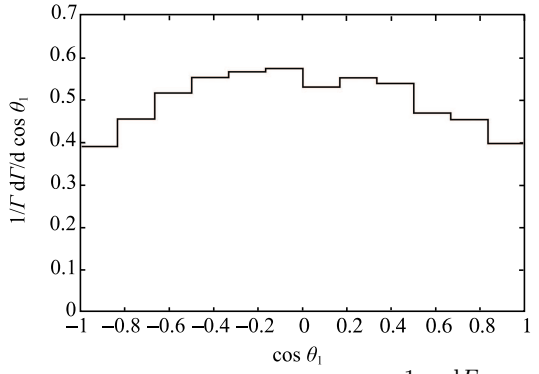

Fig. 6. The normalized distribution $\frac{1}{\Gamma}\frac{{\rm d}\Gamma}{{\rm d}\cos\theta_1}$ vs. $\cos\theta_1$ for a spin-1$^+$ resonance of mass $M_{\rm X}=1.8$ TeV and width $\Gamma_{\rm X}=64.04$ GeV.

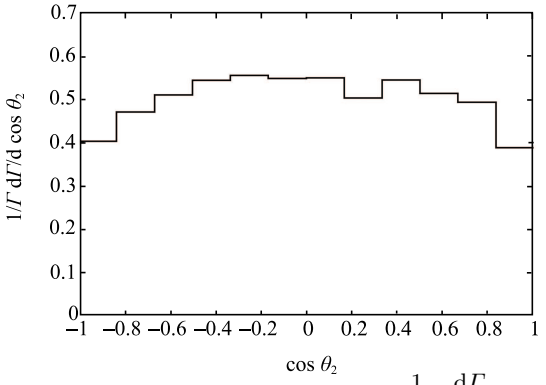

Fig. 7. The normalized distribution $\frac{1}{\Gamma}\frac{{\rm d}\Gamma}{{\rm d}\cos\theta_2}$ vs. $\cos\theta_2$ for a spin-1$^+$ resonance of mass $M_{\rm X}=1.8$ TeV and width $\Gamma_{\rm X}=64.04$ GeV.

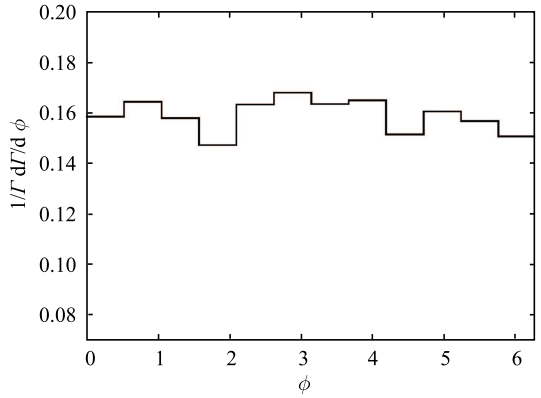

Fig. 8. The normalized distribution $\frac{1}{\Gamma}\frac{\mathrm{d}\Gamma}{\mathrm{d}\phi}$ vs. ϕ for a spin-1^+ resonance of mass $M_{\rm X} = 1.8$ TeV and width $\Gamma_{\rm X} = 64.04$ GeV.

However, while extracting observables one has to take the background processes into account. The $pp \to e^+e^-\mu^+\mu^-$ process is a continuum background to the process $pp \to ZZ \to e^+e^-\mu^+\mu^-$. The effects of the sequential cuts on the background processes for the 14 TeV and 33 TeV 3000 fb^{-1} LHC runs, are shown in Table 6.

Table 6. The effects of the sequential cuts on the simulated background events at 14 TeV and 33 TeV LHC with 3000 fb^{-1} luminosity.

cuts / GeV	14 TeV, 3000 fb^{-1}	33 TeV, 3000 fb^{-1}
Selection cuts	24530	48588
$60 < m_{\rm ee} < 120$	23320	46949
$60 < m_{\mu\mu} < 120$	18468	40082
$1000 < m_{4\rm l}$	41	238

In our simplistic model, we have considered the decays of X to quarks and Z bosons only. Thus we have not considered the effect of the process $X \to \gamma^*\gamma^* \to l_1^+l_1^-l_2^+l_2^-$ in our analysis. In general, models might have such irreducible backgrounds to the process $X \to ZZ \to l_1^+l_1^-l_2^+l_2^-$. However, the cross section to $X \to ZZ \to l_1^+l_1^-l_2^+l_2^-$ will be huge compared to the process $X \to \gamma^*\gamma^* \to l_1^+l_1^-l_2^+l_2^-$. This is because Z being a massive narrow resonance, production of two on-shell Z bosons rather than two off-shell photons is highly favored by the propagator effect. The selection cuts such as $60 < m_{\rm ll} < 120$ etc., will further reduce the cross section of the process $X \to \gamma^*\gamma^* \to l_1^+l_1^-l_2^+l_2^-$. Hence the effect of this process via two off-shell photons will be further suppressed even as a background.

The simulated signal and background events are finally binned in $\cos\theta_1$, $\cos\theta_2$ and ϕ and fitted using Eqs. (26), (27) and (28) integrated over $m^2_{\rm ee}(\equiv q_1^2)$ and $m^2_{\mu\mu}(\equiv q_2^2)$ to obtain the *integrated* angular observables with their respective errors. The values of the observables are tabulated in Table 7 for the two different CM energies.

Table 7. The fit values and the respective errors of the observables T_1, T_2, U_1, U_2, V_1 and V_2 for a spin-1^+ resonance of mass $M_{\rm X} = 1.8$ TeV and width $\Gamma_{\rm X} = 64.04$ GeV at 14 TeV and 33 TeV LHC run (with 3000 fb^{-1} luminosity).

observables	14 TeV, 3000 fb^{-1}	33 TeV, 3000 fb^{-1}
T_2	-0.19 ± 0.11	-0.18 ± 0.06
T_1	0.07 ± 0.09	0.01 ± 0.04
T_2'	-0.09 ± 0.12	-0.10 ± 0.06
T_1'	-0.04 ± 0.10	-0.03 ± 0.05
U_2	0.08 ± 0.51	0.04 ± 0.24
U_1	$(-0.87 \pm 5.33) \times 10^{-1}$	$(-0.17 \pm 2.40) \times 10^{-1}$
V_2	$(-0.41 \pm 5.32) \times 10^{-1}$	$(0.21 \pm 2.36) \times 10^{-1}$
V_1	$(-0.32 \pm 5.11) \times 10^{-1}$	$(0.30 \pm 2.34) \times 10^{-1}$

It is clear from Table 7 that the observables T_2 and T_2', extracted from the $\cos\theta_1$ and $\cos\theta_2$ distributions respectively, match within 1σ error. This is expected since both q_1^2 and q_2^2 are integrated over the same range. A full implementation of the flow chart (shown in Fig. 2) will require a fit with at least two regions $q_1^2 < q_2^2$ and $q_1^2 > q_2^2$. However, given the heavy mass for X the production cross section is low, hence, the errors are still large and more statistics are needed to undertake such a study.

3.2 Study of the angular asymmetries for a spin-1^- resonance

We have so far discussed the possibility of finding a heavy spin-1^+ resonance. However, the resonance may well be a spin-1^-. The limits on the couplings $\tilde{c}_{\rm q}$ and O_1 can also be found from $\sigma \times Br \times \mathcal{A}$ limit from Ref. [29]. In the limit $M_{\rm Z} \ll M_{\rm X}$ and $m_{\rm q} \ll M_{\rm X}$, the coupling $\tilde{c}_{\rm q} \approx c_{\rm q}$ and $O_1 \approx E_1$. Hence, we choose the values $\tilde{c}_{\rm q} = 0.12$ and $O_1 = 7.00 \times 10^{-2}$ for the couplings as a benchmark scenario for our analysis of a spin-1^- resonance of mass 1.8 TeV and decay width $\Gamma_{\rm X} = 64.40$ GeV. We perform the same analysis as given in Sec. 3.1 and extract out the values of the angular observables at two different CM energies, 14 TeV and 33 TeV, at an integrated luminosity of 3000 fb^{-1}. We also find three uni-angular distributions for the spin-1^- resonance, shown in Figs. 9, 10 and 11 respectively. The effects of the sequential cuts are tabulated in Table 8 at 14 TeV and 33 TeV LHC for 3000 fb^{-1} luminosity. The background analysis for a spin-1^- resonance would remain the same as stated in Sec 3.1.

The observables extracted from the uni-angular distributions of the spin-1^-resonance are given in Table 9. Apart from T_2 the errors of the other observables are still not small and require higher statistics to fully study the flowchart in Fig. 2.

If a heavy spin-1 resonance is seen at the LHC, the full angular analysis and the extraction of all the observables may not be entirely possible at a 33 TeV 3000 fb^{-1} run. Once such a resonance is observed, a future high luminosity machine could disentangle the exact spin and parity of the resonance by studying the observables extracted from uni-angular distributions. Moreover, we have not discussed the spin-1 resonance with mixed parity configuration, which would typically require higher statistics to completely disentangle, and is beyond the scope of the current paper.

Table 8. The effects of the sequential cuts on the simulated signal events at 14 TeV 3000 fb^{-1} and 33 TeV 3000 fb^{-1} LHC of a spin-1$^-$ resonance with $M_{\rm X}=1.8$ TeV and width $\Gamma_{\rm X}=64.40$ GeV.

cuts / GeV	14 TeV, 3000 fb^{-1}	33 TeV, 3000 fb^{-1}
selection cuts	220	1155
$60<m_{\rm ee}<120$	200	1154
$60<m_{\mu\mu}<120$	211	1108
$1000<m_{4l}$	210	1105

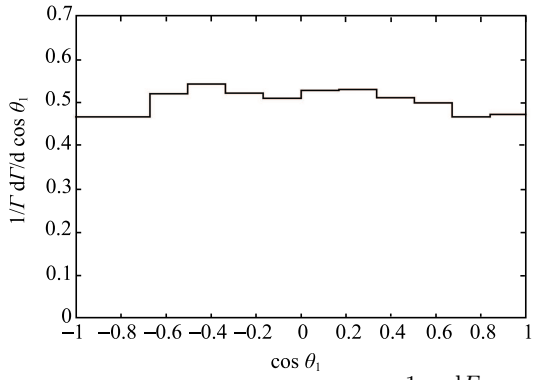

Fig. 9. The normalized distribution $\frac{1}{\Gamma}\frac{{\rm d}\Gamma}{{\rm d}\cos\theta_1}$ vs. $\cos\theta_1$ for a spin-1$^-$ resonance of mass $M_{\rm X}=1.8$ TeV and width $\Gamma_{\rm X}=64.04$ GeV.

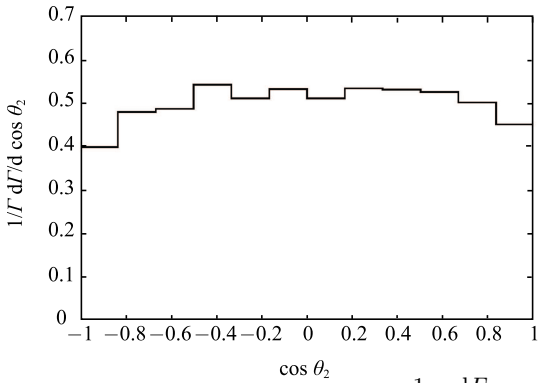

Fig. 10. The normalized distribution $\frac{1}{\Gamma}\frac{{\rm d}\Gamma}{{\rm d}\cos\theta_2}$ vs. $\cos\theta_2$ for a spin-1$^-$ resonance of mass $M_{\rm X}=1.8$ TeV and width $\Gamma_{\rm X}=64.04$ GeV.

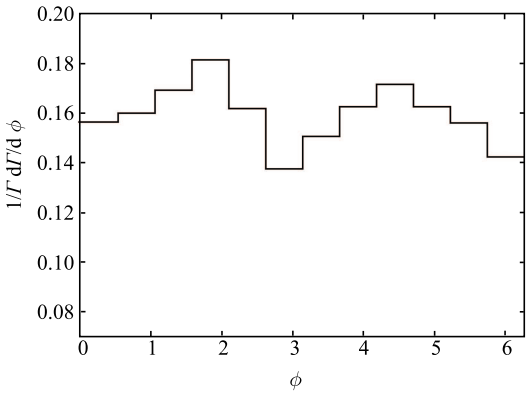

Fig. 11. The normalized distribution $\frac{1}{\Gamma}\frac{{\rm d}\Gamma}{{\rm d}\phi}$ vs. ϕ for a spin-1$^-$ resonance of mass $M_{\rm X}=1.8$ TeV and width $\Gamma_{\rm X}=64.04$ GeV.

Table 9. The fit values and the errors of the observables T_1, T_2, U_1, U_2, V_1 and V_2 for a spin-1$^-$ resonance of mass $M_{\rm X}=1.8$ TeV and width $\Gamma_{\rm X}=64.04$ GeV for signal plus background. The values are extracted for two different CM energies, 14 TeV and 33 TeV LHC runs, with luminosity 3000 fb^{-1}.

observables	14 TeV, 3000 fb^{-1}	33 TeV, 3000 fb^{-1}
T_2	-0.07 ± 0.13	-0.12 ± 0.06
T_1	0.06 ± 0.10	0.01 ± 0.04
T_2'	-0.04 ± 0.13	-0.07 ± 0.06
T_1'	0.09 ± 0.10	-0.01 ± 0.04
U_2	-0.08 ± 0.54	-0.05 ± 0.24
U_1	$(1.99\pm5.16)\times10^{-1}$	$(1.20\pm2.32)\times10^{-1}$
V_2	$(-0.14\pm5.27)\times10^{-1}$	$(0.58\pm2.33)\times10^{-1}$
V_1	$(-0.27\pm5.46)\times10^{-1}$	$(-0.63\pm2.39)\times10^{-1}$

4 Conclusion

We conclude that by looking at three normalized uni-angular distributions for the decay of a resonance to four charged final leptons via two Z bosons, one can infer to a fairly good accuracy the spin and parity of the parent particle. We show that it is possible for a special 2^+ resonance to give angular distributions comparable to those of a 0^+ resonance. It is in this special case that one needs to study the Y^2 dependence of the helicity amplitudes in order to distinguish the two cases. Since the spin-1 case has only two helicity amplitudes, it needs a minimum number of observables to get confirmed or ruled out. We have also provided a step-by-step methodology that must be followed to distinguish the various spin, parity possibilities that are allowed in the case under consideration. A numerical analysis has also been performed for a heavy spin-1 resonance to validate our

formalism. It would therefore not be an overstatement to say that this method can play a crucial role at future high luminosity machines in discovering the spin-parity nature of any new resonance, such as a heavy scalar boson or a Z′ boson or a Kaluza-Klein boson, or any such resonance found to decay to four final charged leptons via two Z bosons.

DS is thankful to HYC and the Institute of Physics, Academia Sinica, Taiwan, for hospitality. We thank Prof. Arjun Menon for many fruitful discussions on this work.

Appendix A

Relationships amongst the form factors and the effective coupling constants

The form factors $E_i^{(J)}, O_i^{(J)}$ (which enter the vertex factors in Eqs. (12), (13) and (14)) are related to the effective coupling constants $e_i^{(J)}, o_i^{(J)}$ (which enter the Lagrangians given in Eqs.(5), (6) and (7)) in the following manner

$$E_1^{(0)} = e_1^{(0)} + 4\,e_2^{(0)}\,(q_1\cdot q_2), \tag{A1}$$

$$E_2^{(0)} = -4\,e_2^{(0)}, \tag{A2}$$

$$O_1^{(0)} = -8\,o_1^{(0)}, \tag{A3}$$

$$O_1^{(1)} = -o_1^{(1)}, \tag{A4}$$

$$E_1^{(1)} = 2e_1^{(1)}, \tag{A5}$$

$$E_1^{(2)} = e_1^{(2)} + \frac{1}{4}e_2^{(2)}(P^2-Q^2) + \frac{1}{16}e_3^{(2)}(P^2-Q^2)^2 + \frac{1}{4}e_4^{(2)}(P^4-(P\cdot Q)^2), \tag{A6}$$

$$E_2^{(2)} = \frac{1}{4}\Big(4e_2^{(2)} + e_3^{(2)}(P^2-Q^2) + 2e_4^{(2)}(P^2+P\cdot Q)\Big), \tag{A7}$$

$$E_3^{(2)} = \frac{1}{4}\left(-2e_2^{(2)} - e_5^{(2)}(P^2-Q^2)\right), \tag{A8}$$

$$E_4^{(2)} = \frac{1}{2}\left(e_3^{(2)} + e_4^{(2)} - 2e_5^{(2)}\right), \tag{A9}$$

$$O_1^{(2)} = 4o_1^{(2)} + o_2^{(2)}(P^2-Q^2) + 2o_3^{(2)}(P^2+P\cdot Q), \tag{A10}$$

$$O_2^{(2)} = o_2^{(2)} + o_3^{(2)}, \tag{A11}$$

$$O_3^{(2)} = -o_1^{(2)}, \tag{A12}$$

$$O_4^{(2)} = o_4^{(2)}. \tag{A13}$$

Appendix B

Helicity amplitudes and partial wave contributions for the decay X → ZZ

If we specify the polarizations of the initial and final particles, then the Feynman amplitude or transition amplitude can always be written in terms of helicity amplitudes. We shall represent the polarisation state of a particle by a ket $|\text{spin}, \text{spin projection to } z \text{ axis}\rangle$. Then the Feynman amplitude for the process

$$\underbrace{|\boldsymbol{J}, J_z\rangle}_{\text{X}} \to \underbrace{|\mathbf{1}, \lambda_1\rangle}_{\text{Z}_1}\,\underbrace{|\mathbf{1}, \lambda_2\rangle}_{\text{Z}_2}$$

is given by the well known expression [36,37] involving the Wigner-D function $\mathscr{D}^{J*}_{J_z\lambda}(\phi,\theta,-\phi)$:

$$\mathscr{M}(J_z,\lambda_1,\lambda_2) = \left(\frac{2J+1}{4\pi}\right)^{\frac{1}{2}} \mathscr{D}^{J*}_{J_z\lambda}(\phi,\theta,-\phi)\,A_{\lambda_1\lambda_2}, \tag{B1}$$

where $\lambda = |\lambda_1 - \lambda_2|$ with $\lambda_{1,2} \in \{\pm 1, 0\}$, $J = |J|$, and $A_{\lambda_1\lambda_2}$ is called the helicity amplitude. Conservation of angular momentum implies that

$$|\lambda| = |\lambda_1 - \lambda_2| \leqslant J. \tag{B2}$$

Since there are no interferences amongst the amplitudes with different helicity configurations, we will have to sum over all the allowed values of λ_1 and λ_2 that are not constrained by the value of J_z after squaring each individual amplitude:

$$|\mathscr{M}|^2 = \sum_{\substack{\lambda_1,\lambda_2 \\ |\lambda_1-\lambda_2|\leqslant J}} |\mathscr{M}(J_z,\lambda_1,\lambda_2)|^2 = \left(\frac{2J+1}{4\pi}\right) \sum_{\substack{\lambda_1,\lambda_2 \\ |\lambda_1-\lambda_2|\leqslant J}} \left|\mathscr{D}^{J*}_{J_z\lambda}(\phi,\theta,-\phi)\right|^2 |A_{\lambda_1\lambda_2}|^2. \tag{B3}$$

Thus the probability of contribution of the helicity amplitude $A_{\lambda_1\lambda_2}$ to the transition amplitude ca be found as $\mathscr{M}(J_z,\lambda_1,\lambda_2)$ is $\left(\frac{2J+1}{4\pi}\right)\left|\mathscr{D}^{J*}_{J_z\lambda}(\phi,\theta,-\phi)\right|^2$. We can therefore write down the following important fact of the helicity amplitude formalism: All the allowed helicity amplitudes for a given decay process contribute, but with different definite probability, to the Feynman amplitude, irrespective of the polarization of the parent (decaying) particle. The probability, however, depends on the polarization of the parent particle and for all allowed helicity amplitudes is non-zero. Since the

two Z bosons are Bose symmetric, the helicity amplitudes satisfy the relation

$$A_{\lambda_2\lambda_1} = (-1)^J A_{\lambda_1\lambda_2} = \begin{cases} +A_{\lambda_1\lambda_2} & \text{for spin-0,2} \\ -A_{\lambda_1\lambda_2} & \text{for spin-1} \end{cases}. \quad \text{(B4)}$$

This relationship is useful in getting the correct number of independent helicity amplitudes. All the allowed helicity amplitudes in the decay X → ZZ are given in Table 10 where N denotes the total number independent helicity amplitudes possible for the particular spin case.

Table B1. Allowed helicity amplitudes considering only the different spin possibilities.

spin of X	allowed helicity amplitudes	N
0	A_{++}, A_{00}, A_{--}.	3
1	$A_{+0} = -A_{0+}$, $A_{0-} = -A_{-0}$.	2
2	A_{++}, A_{00}, A_{--}, $A_{+-} = A_{-+}$, $A_{+0} = A_{0+}$, $A_{0-} = A_{-0}$.	6

It is also known that, if the particle X were a parity eigenstate with eigenvalue $\eta_{\rm X} = +1$ (parity-even) or -1 (parity-odd), then the helicity amplitudes are related by:

$$A_{\lambda_1\lambda_2} = \eta_{\rm X}\,(-1)^J\,A_{-\lambda_1-\lambda_2}. \quad \text{(B5)}$$

The allowed helicity amplitudes for the different spin-parity possibilities can thus be related and are given in Table 11.

Table B2. Relationships amongst the allowed helicity amplitudes for the different spin-parity cases.

J^P of X	allowed helicity amplitudes	N
0^+	$A_{++} = A_{--}$, A_{00}.	2
0^-	$A_{++} = -A_{--}$.	1
1^+	$A_{+0} = -A_{-0} = A_{0-} = -A_{0+}$.	1
1^-	$A_{+0} = A_{-0} = -A_{0-} = -A_{0+}$.	1
2^+	$A_{++} = A_{--}$, A_{00}, $A_{+-} = A_{-+}$, $A_{+0} = A_{-0} = A_{0-} = A_{0+}$.	4
2^-	$A_{++} = -A_{--}$, $A_{+0} = -A_{-0} = -A_{0-} = A_{0+}$.	2

It is clearly evident from above that for the spin-0 case out of the three helicity amplitudes two describe the parity-even scenario and only one describes the parity-odd scenario. Similarly, for spin-1 both parity-even and parity-odd cases are described by one helicity amplitude each. For the spin-2 case, we have four helicity amplitudes describing the parity-even scenario and two helicity amplitudes for the parity-odd scenario.

If we now make a change of basis from the helicity basis to the transversity basis (also called the linear polarization basis), then the number of independent transversity amplitudes must be equal to the number of helicity amplitudes, and all the allowed transversity amplitudes would contribute with definite probability to the Feynman amplitude irrespective of the polarization of the parent (decaying) particle.

Let us now analyse the decay process from the point-of-view of partial wave decompositions. If we describe the two Z boson system by a ket specifying the total spin ($\boldsymbol{L}_{\rm spin}$), the relative orbital angular momentum ($\boldsymbol{L}_{\rm orbital}$), the spin of the parent particle (its $\boldsymbol{J}$ here) and its projection along the direction of flight of one of the Z bosons (J_z): $|\boldsymbol{J}, J_z; \boldsymbol{L}_{\rm orbital}, \boldsymbol{L}_{\rm spin}\rangle$, then

$$\begin{aligned} &\hat{P}_{12}\,|\boldsymbol{J}, J_z; \boldsymbol{L}_{\rm orbital}, \boldsymbol{L}_{\rm spin}\rangle \\ &= (-1)^{L_{\rm orbital}+L_{\rm spin}}\,|\boldsymbol{J}, J_z; \boldsymbol{L}_{\rm orbital}, \boldsymbol{L}_{\rm spin}\rangle\,, \end{aligned} \quad \text{(B6)}$$

where $\hat{P}_{12}$ is the operator that exchanges the two Z bosons (it exchanges both their momenta and spins or polarisations), $L_{\rm orbital}$ and $L_{\rm spin}$ are the modulus of $\boldsymbol{L}_{\rm orbital}$ and $\boldsymbol{L}_{\rm spin}$ respectively. It is obvious that for Bose symmetry to be satisfied $L_{\rm orbital} + L_{\rm spin}$ must be even. The allowed partial waves for the decay X → ZZ are listed in Table 12.

Table B3. Allowed partial waves for all the spin considerations.

$\boldsymbol{L}_{\rm spin}$	$\boldsymbol{L}_{\rm orbital}$	$\boldsymbol{J}$	partial wave
0	**0**	**0**	S-wave
0	**2**	**2**	D-wave
1	**1**	**2**, **1**, **0**	P-wave
1	**3**	**2**	F-wave
2	**0**	**2**	S-wave
2	**2**	**2**, **1**, **0**	D-wave
2	**4**	**2**	G-wave

It is easy to observe that when X has spin-0, then there are three helicity amplitudes and three partial wave contributions (one S-wave, one P-wave and one D-wave). When X has spin-1, then there are only two independent helicity amplitudes and two partial wave contributions (one P-wave and one D-wave). Finally when X has spin-2, then there are six independent helicity amplitudes and six partial wave contributions (one S-wave, one P-wave, two D-waves, one F-wave and one G-wave). It is interesting to note that for the spin-0 case the vertex factor has three form factors, for spin-1 case there are two form factors. However, for the spin-2 case we have eight form factors in the vertex factor instead of six. So one needs to consider only six form factors out of which four should be of parity-even nature and two should be of parity-odd nature. Out of the four parity-odd form factors, only $O_1^{(2)}$ and $O_2^{(2)}$ contribute to the vertex factor as explained in Appendix C.

Appendix C

Redundancy of inclusion of $O_3^{(2)}$, $O_4^{(2)}$ in the spin-2 vertex factor

If we include the $O_3^{(2)}$ term in the vertex factor for spin-2 case, then only the two helicity amplitudes $A_{O1}^{(2)}$ and $A_{O2}^{(2)}$ get modified as follows:

$$A_{\rm O1}^{(2)} = \frac{4Y}{3M_+}\Big(\left(O_1^{(2)} - O_3^{(2)}\right)\left(M_-^4 - M_{\rm X}^2 M_+^2\right)$$

$$+O_2^{(2)}\left(4M_+^2M_{\rm X}^2Y^2\right)\Big), \tag{C1}$$

$$A_{\rm O2}^{(2)}=\frac{8M_1M_2\mu^2Y}{3\sqrt{3}M_+}\left(O_1^{(2)}-O_3^{(2)}\right), \tag{C2}$$

where the previous $O_1^{(2)}$ is now replaced by $\left(O_1^{(2)}-O_3^{(2)}\right)$. Note that only this combination of the two form factors would be accessible to any experiment. Moreover, all other helicity amplitudes remain unchanged. In the vertex factor of Eq. (14) the term which is proportional to $O_4^{(2)}$ can be rewritten using the Schouten identity as follows:

$$\begin{aligned}&\epsilon^{\alpha\beta\rho\sigma}\,Q^\mu Q^\nu q_{1\rho}q_{2\sigma}\\&=\frac{1}{2}\Big[Q^\nu\left(\epsilon^{\alpha\mu\rho\sigma}\,Q^\beta-\epsilon^{\beta\mu\rho\sigma}\,Q^\alpha\right)\\&\quad+Q^\mu\left(\epsilon^{\alpha\nu\rho\sigma}\,Q^\beta-\epsilon^{\beta\nu\rho\sigma}\,Q^\alpha\right)\Big]q_{1\rho}q_{2\sigma}\\&\quad-\frac{Q^2}{4}\left(\epsilon^{\alpha\beta\mu\rho}\,P_\rho Q^\nu+\epsilon^{\alpha\beta\nu\rho}\,P_\rho Q^\mu\right)\\&\quad+\frac{P\cdot Q}{4}\left(\epsilon^{\alpha\beta\mu\sigma}\,Q^\nu Q_\sigma+\epsilon^{\alpha\beta\nu\sigma}\,Q^\mu Q_\sigma\right).\end{aligned} \tag{C3}$$

Thus the form factor $O_4^{(2)}$ can be absorbed into the existing form factors $O_2^{(2)}$ and $O_3^{(2)}$ by redefining them as follows:

$$O_2^{(2)}\to O_2^{(2)}+\frac{1}{2}O_4^{(2)}, \tag{C4}$$

$$O_3^{(2)}\to O_3^{(2)}-\frac{Q^2}{4}O_4^{(2)}. \tag{C5}$$

The remaining contribution of $O_4^{(2)}$ is proportional to $P\cdot Q$. Since $P\cdot Q$ is not Bose symmetric, this term does not contribute to our vertex factor. Therefore the effect of including the $O_3^{(2)}$ and $O_4^{(2)}$ terms in the vertex factor can simply be taken care of by the following redefinitions of $O_1^{(2)}$ and $O_2^{(2)}$ as follows:

$$O_1^{(2)}\to O_1^{(2)}-O_3^{(2)}+\frac{Q^2}{4}O_4^{(2)}, \tag{C6}$$

$$O_2^{(2)}\to O_2^{(2)}+\frac{1}{2}O_4^{(2)}. \tag{C7}$$

Since we cannot have more than six helicity amplitudes for the spin-2 case, and we already have six form factors in the vertex factor, any additional form factor that we introduce in the vertex factor must come in association with the existing form factors, as proved here.

Appendix D

Expressions for $T_i^{(J)}$, $T_i^{\prime(J)}$, $U_i^{(J)}$, $V_i^{(J)}$

The expressions for the coefficients $T_i^{(J)}$, $T_i^{\prime(J)}$, $U_i^{(J)}$, $V_i^{(J)}$ that entered the uni-angular distributions are given as follows:

$$T_1^{(0)}=-T_1^{\prime(0)}=-\frac{3}{2}\eta\,{\rm Re}\left(F_{E2}^{(0)}F_{O1}^{(0)*}\right), \tag{D1}$$

$$T_2^{(0)}=T_2^{\prime(0)}=\frac{1}{4}\left(1-3\left|F_{E1}^{(0)}\right|^2\right), \tag{D2}$$

$$U_1^{(0)}=-\frac{9\pi^2}{32\sqrt{2}}\eta^2\,{\rm Re}\left(F_{E1}^{(0)}F_{E2}^{(0)*}\right), \tag{D3}$$

$$U_2^{(0)}=\frac{1}{4}\left(\left|F_{E2}^{(0)}\right|^2-\left|F_{O1}^{(0)}\right|^2\right), \tag{D4}$$

$$V_1^{(0)}=-\frac{9\pi^2}{32\sqrt{2}}\eta^2\,{\rm Im}\left(F_{E1}^{(0)}F_{O1}^{(0)*}\right), \tag{D5}$$

$$V_2^{(0)}=\frac{1}{2}\,{\rm Im}\left(F_{E2}^{(0)}F_{O1}^{(0)*}\right), \tag{D6}$$

$$T_1^{(1)}=-\frac{6\sqrt{2}\eta M_{\rm X}^3M_1^2Y}{D_1D_2}\left(M_{\rm X}^2-M_1^2+3M_2^2\right){\rm Re}\left(F_{E1}^{(1)}F_{O1}^{(1)*}\right), \tag{D7}$$

$$T_1^{\prime(1)}=\frac{6\sqrt{2}\eta M_{\rm X}^3M_2^2Y}{D_1D_2}\left(M_{\rm X}^2+3M_1^2-M_2^2\right){\rm Re}\left(F_{E1}^{(1)}F_{O1}^{(1)*}\right), \tag{D8}$$

$$\begin{aligned}T_2^{(1)}=-2M_{\rm X}^2Y^2\Bigg(&\frac{\left|F_{O1}^{(1)}\right|^2}{D_1^2}\Big(\left(M_{\rm X}^2-M_1^2\right)\left(M_1^2+4M_2^2\right)+2M_2^4\Big)\\&+\frac{2\left|F_{E1}^{(1)}\right|^2}{D_2^2}\Big(M_{\rm X}^2\left(M_1^2+16M_2^2\right)-M_2^2\left(20M_1^2-3M_2^2\right)\Big)\Bigg),\end{aligned} \tag{D9}$$

$$\begin{aligned}T_2^{\prime(1)}=-2M_{\rm X}^2Y^2\Bigg(&\frac{\left|F_{O1}^{(1)}\right|^2}{D_1^2}\Big(\left(M_{\rm X}^2-M_2^2\right)\left(4M_1^2+M_2^2\right)+2M_1^4\Big)\\&+\frac{2\left|F_{E1}^{(1)}\right|^2}{D_2^2}\Big(M_{\rm X}^2\left(16M_1^2+M_2^2\right)-M_1^2\left(20M_2^2-3M_1^2\right)\Big)\Bigg),\end{aligned} \tag{D10}$$

$$\begin{aligned}U_1^{(1)}=&\frac{9\pi^2\eta^2M_{\rm X}^2M_1M_2}{16D_1^2D_2^2}\Big(4\left|F_{O1}^{(1)}\right|^2M_{\rm X}^2Y^2\Big(16M_{\rm X}^6M_+^2\\&+M_{\rm X}^4\left(56M_+^4-85M_-^4\right)+M_{\rm X}^2\left(96M_+^2M_-^4-86M_+^6\right)\\&-35M_+^4M_-^4+38M_-^8\Big)\\&-\left|F_{E1}^{(1)}\right|^2\Big(\left(M_{\rm X}^2-2M_+^2\right)^2-M_-^4\Big)\Big(4M_{\rm X}^6M_+^2\\&-M_{\rm X}^4\left(5M_+^4+M_-^4\right)\\&+12M_{\rm X}^2M_+^2\left(M_+^4-M_-^4\right)+3M_+^4M_-^4-M_-^8\Big)\Big),\end{aligned} \tag{D11}$$

$$U_2^{(1)}=-\frac{8M_1^2M_2^2M_-^4}{D_2^2}\left|F_{E1}^{(1)}\right|^2, \tag{D12}$$

$$\begin{aligned}V_1^{(1)}=&-\frac{9\pi^2\eta^2M_{\rm X}M_1M_2Y}{2\sqrt{2}D_1D_2}\left(M_{\rm X}^4-2M_{\rm X}^2M_+^2-M_-^4\right)\\&\times{\rm Im}\left(F_{E1}^{(1)}F_{O1}^{(1)*}\right),\end{aligned} \tag{D13}$$

$$V_2^{(1)}=0, \tag{D14}$$

$$\begin{aligned}T_1^{(2)}=&-\frac{3\eta}{2M_+^2\mu^2\nu^2}\Big(2M_{\rm X}M_+^3\nu^2\,{\rm Re}\left(F_{E2}^{(2)}F_{O2}^{(2)*}\right)\\&+M_1^2\mu^2\nu^2\,{\rm Re}\left(F_{E3}^{(2)}F_{O1}^{(2)*}\right)+M_2M_-^2\end{aligned}$$

$$\times\left(\sqrt{3}M_1\nu^2\,\mathrm{Re}\left(F_{E3}^{(2)}F_{O2}^{(2)*}\right)+M_1\mu^2\,\mathrm{Re}\left(F_{E4}^{(2)}F_{O1}^{(2)*}\right)\right.$$
$$\left.+\sqrt{3}M_2M_-^2\,\mathrm{Re}\left(F_{E4}^{(2)}F_{O2}^{(2)*}\right)\right)\Big), \tag{D15}$$

$$T_1'^{(2)}=\frac{3\eta}{2M_+^2\mu^2\nu^2}\Big(2M_{\rm X}M_+^3\nu^2\,\mathrm{Re}\left(F_{E2}^{(2)}F_{O2}^{(2)*}\right)$$
$$+M_2^2\mu^2\nu^2\,\mathrm{Re}\left(F_{E3}^{(2)}F_{O1}^{(2)*}\right)+M_1M_-^2$$
$$\times\left(-\sqrt{3}M_2\nu^2\,\mathrm{Re}\left(F_{E3}^{(2)}F_{O2}^{(2)*}\right)-M_2\mu^2\,\mathrm{Re}\left(F_{E4}^{(2)}F_{O1}^{(2)*}\right)\right)$$
$$+\left(\sqrt{3}M_1^2M_-^4\,\mathrm{Re}\left(F_{E4}^{(2)}F_{O2}^{(2)*}\right)\right)\Big), \tag{D16}$$

$$T_2^{(2)}=\frac{1}{4}\Big(-2\left|F_{E1}^{(2)}\right|^2+\left|F_{E2}^{(2)}\right|^2$$
$$+\left(\left|F_{E3}^{(2)}\right|^2+\left|F_{O1}^{(2)}\right|^2\right)\left(\frac{M_1^2-2M_2^2}{M_+^2}\right)$$
$$+\left|F_{E4}^{(2)}\right|^2\left(2M_{\rm X}^2\frac{M_+^2}{\nu^4}+\frac{M_-^4}{M_+^2\nu^4}\left(M_2^2-2M_1^2\right)\right)$$
$$+\left|F_{O2}^{(2)}\right|^2\left(4M_{\rm X}^2\frac{M_+^2}{\mu^4}+3\frac{M_-^4}{M_+^2\mu^4}\left(M_2^2-2M_1^2\right)\right)$$
$$+\frac{6M_1M_2M_-^2}{M_+^2\mu^2\nu^2}\Big(\mu^2\,\mathrm{Re}\left(F_{E3}^{(2)}F_{E4}^{(2)*}\right)$$
$$+\sqrt{3}\nu^2\,\mathrm{Re}\left(F_{O1}^{(2)}F_{O2}^{(2)*}\right)\Big)\Big), \tag{D17}$$

$$T_2'^{(2)}=\frac{1}{4}\Big(-2\left|F_{E1}^{(2)}\right|^2+\left|F_{E2}^{(2)}\right|^2$$
$$+\left(\left|F_{E3}^{(2)}\right|^2+\left|F_{O1}^{(2)}\right|^2\right)\left(\frac{M_2^2-2M_1^2}{M_+^2}\right)$$
$$+\left|F_{E4}^{(2)}\right|^2\left(2M_{\rm X}^2\frac{M_+^2}{\nu^4}+\frac{M_-^4}{M_+^2\nu^4}\left(M_1^2-2M_2^2\right)\right)$$
$$+\left|F_{O2}^{(2)}\right|^2\left(4M_{\rm X}^2\frac{M_+^2}{\mu^4}+3\frac{M_-^4}{M_+^2\mu^4}\left(M_1^2-2M_2^2\right)\right)$$
$$-\frac{6M_1M_2M_-^2}{M_+^2\mu^2\nu^2}\Big(\mu^2\,\mathrm{Re}\left(F_{E3}^{(2)}F_{E4}^{(2)*}\right)$$
$$+\sqrt{3}\nu^2\,\mathrm{Re}\left(F_{O1}^{(2)}F_{O2}^{(2)*}\right)\Big)\Big), \tag{D18}$$

$$U_1^{(2)}=\frac{9\pi^2\eta^2}{64M_+^2\mu^4\nu^4}\Big(\sqrt{2}M_+^2\mu^4\nu^4\,\mathrm{Re}\left(F_{E1}^{(2)}F_{E2}^{(2)*}\right)$$
$$-M_-^4\mu^4\nu^2\,\mathrm{Re}\left(F_{E3}^{(2)}F_{E4}^{(2)*}\right)+\left|F_{E3}^{(2)}\right|^2M_1M_2\mu^4\nu^4$$
$$-\left|F_{E4}^{(2)}\right|^2M_1M_2M_-^4\mu^4+\sqrt{3}M_-^4\mu^2\nu^4\,\mathrm{Re}\left(F_{O1}^{(2)}F_{O2}^{(2)*}\right)$$
$$-\left|F_{O1}^{(2)}\right|^2M_1M_2\mu^4\nu^4+3\left|F_{O2}^{(2)}\right|^2M_1M_2M_-^4\nu^4\Big), \tag{D19}$$

$$U_2^{(2)}=\frac{1}{4}\left|F_{E2}^{(2)}\right|^2-\frac{M_{\rm X}^2M_+^2}{\mu^4}\left|F_{O2}^{(2)}\right|^2, \tag{D20}$$

$$V_1^{(2)}=\frac{9\pi^2\eta^2}{64M_+^2\mu^2\nu^2}\Big(2\sqrt{2}M_{\rm X}M_+^3\nu^2\,\mathrm{Im}\left(F_{E1}^{(2)}F_{O2}^{(2)*}\right)$$
$$+2M_1M_2\mu^2\nu^2\,\mathrm{Im}\left(F_{E3}^{(2)}F_{O1}^{(2)*}\right)$$
$$-\sqrt{3}M_-^4\nu^2\,\mathrm{Im}\left(F_{E3}^{(2)}F_{O2}^{(2)*}\right)$$
$$-M_-^4\mu^2\,\mathrm{Im}\left(F_{E4}^{(2)}F_{O1}^{(2)*}\right)$$
$$-2\sqrt{3}M_-^4M_1M_2\,\mathrm{Im}\left(F_{E4}^{(2)}F_{O2}^{(2)*}\right)\Big), \tag{D21}$$

$$V_2^{(2)}=M_{\rm X}\frac{M_+}{\mu^2}\,\mathrm{Im}\left(F_{E2}^{(2)}F_{O2}^{(2)*}\right). \tag{D22}$$

Here η is defined as

$$\eta=\frac{2\,v_{\rm l}\,a_{\rm l}}{v_{\rm l}^2+a_{\rm l}^2}, \tag{D23}$$

with $v_{\rm l}=2I_{3{\rm l}}-4e_{\rm l}\,\sin^2\theta_{\rm W}$ and $a_{\rm l}=2I_{3{\rm l}}$. In the present case $v_{\rm l}=-1+4\sin^2\theta_{\rm W}$ and $a_{\rm l}=-1$. Substituting the value $\sin^2\theta_{\rm W}=0.231$, we get $\eta=0.151$.

References

1 G. Aad et al (ATLAS Collaboration), Phys. Lett. B, **716**: 1 (2012); arXiv:1207.7214 [hep-ex]
2 S. Chatrchyan et al (CMS Collaboration), Phys. Lett. B, **716**: 30 (2012); arXiv:1207.7235 [hep-ex]
3 A. Menon, T. Modak, D. Sahoo, R. Sinha and H. Y. Cheng, Phys. Rev. D, **89**: 095021 (2014): arXiv:1301.5404 [hep-ph]
4 C. A. Nelson, Phys. Rev. D, **30**: 1937 (1984)
5 J. R. Dell'Aquila and C. A. Nelson, Phys. Rev. D, **33**: 80 (1986)
6 C. A. Nelson, Phys. Rev. D, **37**: 1220 (1988)
7 D. J. Miller, S. Y. Choi, B. Eberle, M. M. Muhlleitner and P. M. Zerwas, Phys. Lett B, **505**: 149 (2001); hep-ph/0102023
8 S. Y. Choi, Measuring the spin of the Higgs bosons, in 10th International Conference on Supersymmetry, Edited by P. Nath, P. M. Zerwas, C. Grosche. Hamburg, DESY, 2002
9 S. Y. Choi, D. J. Miller, M. M. Muhlleitner and P. M. Zerwas, Phys. Lett. B, **553**: 61 (2003); hep-ph/0210077
10 Y. Gao, A. V. Gritsan, Z. Guo, K. Melnikov, M. Schulze and N. V. Tran, Phys. Rev. D, **81**: 075022 (2010); arXiv:1001.3396 [hep-ph]
11 M. Kramer, J. H. Kuhn, M. L. Stong and P. M. Zerwas, Z. Phys. C, **64**: 21 (1994); hep-ph/9404280
12 C. P. Buszello, I. Fleck, P. Marquard and J. J. van der Bij, Eur. Phys. J. C, **32**: 209 (2004); hep-ph/0212396
13 M. Bluj, CMS-NOTE-2006-094
14 O. J. P. Eboli, C. S. Fong, J. Gonzalez-Fraile and M. C. Gonzalez-Garcia, Phys. Rev. D, **83**: 095014 (2011); arXiv:1102.3429 [hep-ph]
15 D. Stolarski and R. Vega-Morales, Phys. Rev. D, **86**: 117504 (2012); arXiv:1208.4840 [hep-ph]
16 S. Bolognesi, Y. Gao, A. V. Gritsan, K. Melnikov, M. Schulze, N. V. Tran and A. Whitbeck, Phys. Rev. D, **86**: 095031 (2012); arXiv:1208.4018 [hep-ph]
17 T. Han, J. D. Lykken and R. -J. Zhang, Phys. Rev. D, **59**: 105006 (1999); hep-ph/9811350
18 J. S. Gainer, J. Lykken, K. T. Matchev, S. Mrenna and M. Park, arXiv:1403.4951 [hep-ph]
19 W. -Y. Keung, I. Low and J. Shu, Phys. Rev. Lett., **101**: 091802 (2008); arXiv:0806.2864 [hep-ph]
20 P. Langacker, Rev. Mod. Phys., **81**: 1199 (2009); arXiv:0801.1345 [hep-ph]
21 T. Flacke, A. Menon and Z. Sullivan, Phys. Rev. D, **86**: 093006 (2012); arXiv:1207.4472 [hep-ph]

22 P. Avery, D. Bourilkov, M. Chen, T. Cheng, A. Drozdetskiy, J. S. Gainer, A. Korytov and K. T. Matchev et al, Phys. Rev. D, **87**, (5): 055006 (2013); arXiv:1210.0896 [hep-ph]

23 J. S. Gainer, J. Lykken, K. T. Matchev, S. Mrenna and M. Park, Phys. Rev. Lett., **111**: 041801 (2013); arXiv:1304.4936 [hep-ph]

24 M. Chen, T. Cheng, J. S. Gainer, A. Korytov, K. T. Matchev, P. Milenovic, G. Mitselmakher and M. Park et al, Phys. Rev. D, **89**, (3): 034002 (2014); arXiv:1310.1397 [hep-ph]

25 K. Cheung and T. -C. Yuan, Phys. Rev. Lett., **108**: 141602 (2012); arXiv:1112.4146 [hep-ph]

26 G. F. Giudice, R. Rattazzi and J. D. Wells, Nucl. Phys. B, **544**: 3 (1999); hep-ph/9811291

27 K. Hagiwara, J. Kanzaki, Q. Li and K. Mawatari, Eur. Phys. J. C, **56**: 435 (2008); arXiv:0805.2554 [hep-ph]

28 P. Artoisenet, P. de Aquino, F. Demartin, R. Frederix, S. Frixione, F. Maltoni, M. K. Mandal and P. Mathews et al, JHEP, **1311**: 043 (2013); arXiv:1306.6464 [hep-ph]

29 V. Khachatryan et al [CMS Collaboration], Phys. Rev. D, **91**, (5): 052009 (2015); arXiv:1501.04198 [hep-ex]

30 J. Alwall, M. Herquet, F. Maltoni, O. Mattelaer and T. Stelzer, JHEP, **1106**: 128 (2011); arXiv:1106.0522 [hep-ph]

31 T. Sjostrand, L. Lonnblad, S. Mrenna and P. Z. Skands, hep-ph/0308153.

32 J. de Favereau et al (DELPHES 3 Collaboration), JHEP, **1402**: 057 (2014); arXiv:1307.6346 [hep-ex]

33 J. Pumplin, D. R. Stump, J. Huston, H. L. Lai, P. M. Nadolsky and W. K. Tung, JHEP, **0207**: 012 (2002); arXiv:hep-ph/0201195

34 ATLAS Collaboration, "Measurements of the properties of the Higgs-like boson in the four lepton decay channel with the ATLAS detector using 25 fb^{-1} of proton-proton collision data"ATLAS-CONF-2013-013

35 G. Aad et al (ATLAS Collaboration), arXiv:0901.0512 [hep-ex]

36 M. Jacob and G. C. Wick, Annals Phys., **7**: 404 (1959); Annals Phys, **281**: 774 (2000)

37 Suh-Urk Chung, Spin formalisms, Updated Version, Brookhaven Nat. Lab., Upton, NY, 2008. This report is an updated version of CERN-71-08